Structure and Mechanics of Non-piscine Control Surfaces

Frank E. Fish

Abstract— **Animals display a variety of control surfaces that can be used for propulsion and maneuvering devises. For non-piscine vertebrates, these control surfaces are primarily evolutionary modifications of the paired appendages (i.e., legs). The diversity of control surfaces can be classified with regard to the forces used for stability and maneuverability. For animals, the pertinent forces are pressure drag, acceleration reaction, and lift. These forces can be generated actively by motion of the control surfaces, or passively from flows produced by movements of the body or external flow fields. Drag-based control surfaces are associated with paddling and rowing movements, where the limbs are oriented either in the vertical parasagittal plane or horizontal plane, respectively. The paddle is unstreamlined and has a triangular design with a broad distal end; thereby, affecting a large mass of water Appendages, which are used to generate lift-based forces, are relatively stiff hydrofoils. To maximize lift, the hydrofoil should have a crescent, wing-like design with high aspect ratio. This shape provides the hydrofoil with a high lift-to-drag ratio and high propulsive efficiency. The tail flukes of cetaceans are streamlined control surfaces with a wing-like design. The flukes of cetaceans function in the hydrodynamic generation of forces for thrust, stability, and maneuverability. The three-dimensional geometry of flukes is associated with the production of lift and drag. Previous studies of fluke geometry have been limited in the number of species examined and the resolution of measurements.**

Index Terms—**control surface, design, flippers, hydrodynamics**

I. SURVEY OF ORGANISMS

a. Non-piscine swimmers

Exclusive of fish, the taxonomic list of aquatic animals that use control surfaces for stabilizing the body, maintaining trim, station-holding, maneuvering, and propulsion include amphibians, reptiles, birds, mammals, and cephalopod mollusks.

Within the amphibians, frogs swim using a simultaneous rowing action of the two hind feet, which have become expanded with an interdigital webbing [1], [2]. No analysis has been undertaken to examine maneuverability in frogs.

Manuscript submitted June 8, 2003. This work was supported by the Office of Naval Research under Grant N000140310004 (sponsor Dr. Promode Bandyopadhyay).

F. E. Fish is with the Department of Biology, West Chester University, West Chester, PA 19383 USA (phone: 610-436-2460; fax: 610-436-2183; e-mail: ffish@wcupa.edu).

Within the reptiles, there are a variety of aquatic and semi-aquatic species of turtles (Order Chelonia) that use paired appendages for swimming and maneuvering. Aquatic propulsion is effected by alternate rowing motions of the four paddle-like feet in semi-aquatic, freshwater turtles [3], [4]. For propulsion, sea turtles use a wing-like motion of the two forelegs which have been modified as flippers [5]-[8].

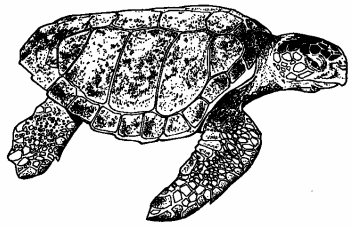

Fig. 1. Sea turtle showing modification of foreflippers.

In addition to swimming reptiles that exists today, there were a number of aquatic groups that occurred at a time when dinosaurs inhabited the earth (245-65 million years ago) and have since become extinct. As with dinosaurs, these marine reptiles grew to a large body size. These groups included the ichthyosaurs (order Ichthyosauria), mosasaurs (order Squamata: family Mosasauridae), plesiosaurs and nothosaurs (order Sauropterygia), placodonts (order Placodontia), and sea turtles (order Chelonia: family Protostegidae) [9], [10]. The ichthyosaurs used body and tail undulations to swim (Fig. 2). In early ichthyosaurs, the propulsive movements were eel-like, but more derived species developed a high aspect ratio tail and fusiform body that were analogous with respect to swimming motion and habits to sharks and dolphins [11]-[15]. Highly derived species of ichthyosaurs had paired pectoral and pelvic flippers and a dorsal fin resembling the control surfaces of modern dolphins. Mosasaurs were elongate aquatic lizards which ranged in size from 4 to 15 m long. These extinct relatives to modern monitor lizards swam by undulation of a long, broad tail. Paddle-like pectoral and pelvic appendages were present and may have functioned in maneuvers. Swimming by plesiosaurs is the least understood, because these animals lack modern relatives with similar anatomical designs and habits. The body was highly fusiform, although slightly compressed, with the head being large with a short neck or small with a long neck (Fig. 2). The fore and hind limbs were modified as high aspect ratio wing-like flippers [16]-[20]. It is believed that plesiosaurs swam with wing-like

motions rather than rowing or paddling, but the pattern of movement between the four limbs is unknown.

Fig. 2. Plesiosaur skeleton showing wing-like pectoral and pelvic flippers.

A number of bird species are cable of swimming including penguins (order Sphenisciformes), loons (order Gaviiformes), grebes (order Procellariiformes), pelicans and cormorants (order Pelecaniformes), ducks, geese and swans (order Anseriformes), and gulls, auks, and puffins (order Charadriiformes). The dominant form of swimming is paddling at the water surface. Paddling uses alternate strokes of the webbed hind feet as exemplified by ducks [21]-[23]. Winged swimming is used by puffins and penguins. Puffins and their relatives use the wings for both swimming and flight [24]. In penguins, the wings are used exclusively for swimming and have taken on a high aspect ratio design (Fig. 3) [25]-[29].

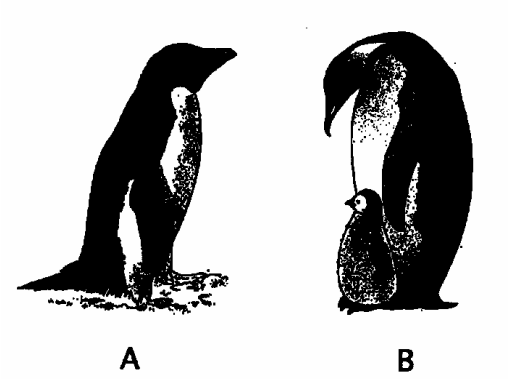

Fig. 3. Penguins. (A) Adélie penguin and (B) Emperor penguin.

A variety of mammalian lineages have secondarily invaded the water (Fig. 4-6) [11], [30]. Highly derived aquatic mammals are found in the taxonomic orders Cetacea (whales, dolphins, porpoises), Pinnipedia (seals, sea lions, fur seals, walrus), and Sirenia (manatees, dugong). The cetaceans are divided into two groups, the baleen whales (Mysticete) and toothed whales (Odontocete). Less derived mammals which have lifestyles tied to the water are semi-aquatic from a wide range of mammalian orders including Monotremata (platypus), Marsupialia (water opossum), Insectivora (water shrew, desman, otter shrew), Carnivora (otters, polar bear), Rodentia (beaver, muskrat, nutria), Lagomorpha (marsh rabbit), Perissodactyla (tapir), and Artiodactyla (hippopotamus). Most semi-aquatic mammals swim by paddling or rowing with webbed feet (Fig. 4) [30]. Paddling is confined to swimming at the surface, whereas rowing motions are used when submerged to aid in thrust production and dynamic buoyancy control [31]-[37]. Typically, the pelvic appendages are used by semi-aquatic mammals for propulsion and maneuvering. The pectoral limbs are used for swimming and turning in water by the polar bear. The platypus rows using its webbed forelimbs [34], [37]. Although propulsion is mainly produced by paddling and undulation of the hind feet and tail in river otters (*Lutra canadensis*), respectively, the forelimbs are used during maneuvers [38].

Fig. 4. Sea otter showing paddle-like hind feet.

Marine mammals, including the orders Pinnipedia, Cetacea, and Sirenia, are the most adapted to the aquatic environment. The control surfaces of marine mammals are used for propulsion and maneuvers (Fig. 5, 6; [12], [30], [39]-[45].

The foreflippers, used by the pinnipeds (e.g., sea lions), act as oscillatory hydrofoils [37]. Both fore- and hind flippers (Fig. 5) are used for turning [46]. Lift-based oscillations also generate thrust from dorsoventral movements by the caudal flukes of cetaceans and sirenians [47]-[51] or from lateral movements of the paired hind flippers by the Phocidae and Odobenidae [41], [52]-[55]. Lift-based oscillation, exclusive of the otariid pinnipeds, is analogous to the thunniform mode of fishes which represents the advanced end of a continuum of undulatory swimming modes [56], [57]. In this mode, undulations of the body are transmitted to the oscillatory hydrofoil through mobile joints. These joints control the angle of attack of the hydrofoil to maintain lift and thrust throughout the stroke cycle [41], [56].

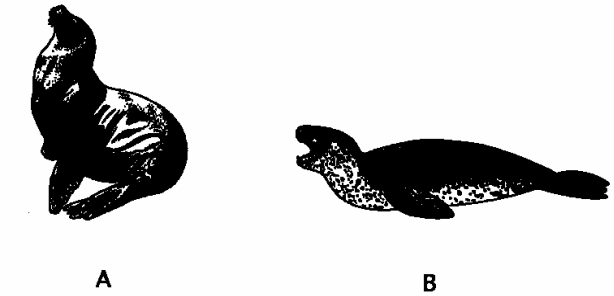

Fig. 5. Pinnipeds showing difference in pectoral and pelvic flippers for (A) Otariid sea lion and (B) Phocid leopard seal.

For cetaceans, the control surfaces consist of the pectoral flippers, dorsal fin, compressed caudal peduncle, and caudal flukes (Fig. 6). The pectoral flippers, caudal peduncle, and caudal flukes are mobile and provide the main contribution to lateral turning, diving, and surfacing [58]-[62]. The broad peduncle and flukes at the end of the tail serve collectively as a rudder to produce turns. During turns, the tail can be twisted rotating the flukes up to 88^o [62]. Dorsal fins are not mobile. The position of the dorsal fin aft of the center of gravity is important for stability [47], [63], [64]. The fin resists yawing and rolling motion and acts to prevent side-slip during turning maneuvers [62]. The beluga whale (*Delphinapterus leucas*) lacks a dorsal fin and turns by rolling the body by 90^o [62].

Sirenians, including manatees and dugongs have few control surfaces with only two mobile pectoral flippers and the tail fluke. These herbivorous mammals are generally slow moving [48]. Manatees are able to precisely maneuver using the mobile paddle-like pectoral flippers in combination with an ability to hydrostatically control body trim [65].

Convergent with the control surfaces exhibited by various aquatic vertebrates, cephalopod mollusks display a range of fins that can act to stabilize the animal trajectory (Fig.7). In various species the fins can be undulated for propulsion at low speeds, whereas, high-speed swimming is performed by jet propulsion [66]. When jetting, the fins typically are positioned anteriorly. The arms can be used also as control surfaces to provide lift for directional control [66]. During attacks on fish, the orientation may be reversed with the fins posteriorly situated. These head-first attacks have maximum speeds of 2.4 to 2.6 m/s with accelerations up to 5.6 m/s^2 [67]. In flying squid, the fins are used as canards in concert with the laterally extended arms during gliding flight [68].

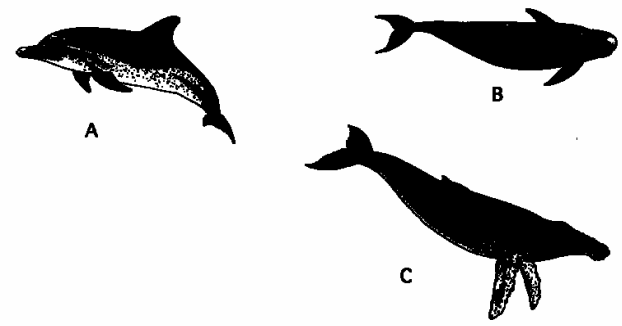

Fig. 6. Cetaceans exhibiting control surfaces of the pectoral flippers, dorsal fin, caudal peduncle, and caudal flukes. (A) Spotted dolphin, (B) Pilot whale, and (C) humpback whale.

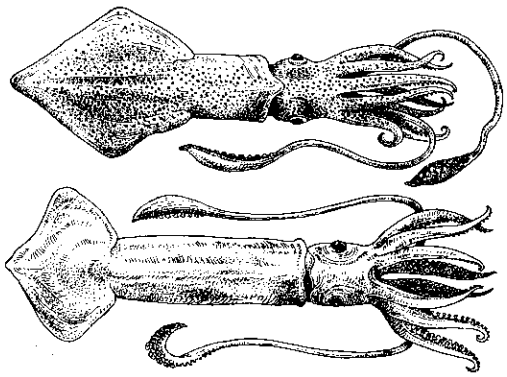

Fig. 7. Squid displaying lateral fins.

b. Paddle vs. hydrofoil

The diversity of control surfaces can be classified with regard to the forces used for stability and maneuverability. For animals, the pertinent forces are pressure drag, acceleration reaction, and lift [30], [42], [69]-[71]. These forces can be generated actively by motion of the control surfaces, or passively from flows produced by movements of the body or external flow fields.

Pressure drag is a resultant of the asymmetry of the fore and aft flow around an appendage. This asymmetry creates a pressure difference which is the basis of the drag. Drag-based control surfaces are associated with paddling and rowing movements, where the limbs are oriented either in the vertical parasagittal plane or horizontal plane, respectively. The paddle is unstreamlined and has a triangular design with a broad distal end; thereby, increasing propulsive efficiency by affecting a large mass of water [72], [73]. In addition, the narrow attachment of the triangular paddle with the body reduces drag due to interference between body and propulsor. The paddle has a stroke cycle that is divided into power and recovery phases [2], [36], [74]. During the power phase, paddle is swept in a direction opposite to the direction of the drag vector (Fig. 8). Depending on the direction of motion, the paddle can be used to provide an anterior thrust, a braking action, reversal of swimming direction, or a turning moment if used asymmetrically. The recovery phase repositions the appendage. To prevent an oppositely applied pressure drag on the paddle that will negate the force and movement generated, the paddle is collapsed or feathered (Fig.8). Examples of drag-based paddlers include labriform fish, frogs, turtles, ducks, semi-aquatic mammals, and manatees. Paddling is associated with slow surface swimming and precise maneuverability.

Acceleration reaction results from changes in the kinetic energy of water accelerated by action of the propulsive body structure [70], [75]. The acceleration reaction is dependent on an additional inertial mass, the added mass, that when

added to the inertia of the body accelerating in the water balances the momentum changes [75], [76]. The acceleration reaction differs from drag in that (1) the acceleration reaction is directly proportional to the volume of an object, while drag is proportional to the surface or cross-sectional area, and (2) the acceleration reaction depends on changes in velocity of an object, resisting both acceleration and deceleration, while drag depends on the instantaneous velocity of the object, resisting acceleration but augmenting deceleration [75]. Some resistive drag accompanies this mode of force generation due to viscous effects. Animals which swim by undulation of appendages (Ostraciiform, Gymnotiform, Balistiform, Rajiform, and Diodontiform fish) use the acceleration reaction [56], [70], [76], [77]. Flattening of the undulatory surface enhances the magnitude of inertial effects [12], [78]-[80]. Control surfaces using undulations are typically broad based [56], [57]. Because undulations can be generated continuously by the swimmer, force production is constant.

Use of the acceleration reaction is constrained by size [70]. As animals get larger, the ability of the muscle to generate force relative to inertial forces decreases [76].

Acceleration reaction is used also for jet propulsion [75]. Thrust results from the forceful expulsion of a mass of water from some internal cavity. Squids are capable of some maneuvering control by directing the jet.

Appendages, which are used to generate lift-based forces, are relatively stiff hydrofoils. To maximize lift, the hydrofoil should have a crescent, wing-like design with high aspect ratio (span^2 / area) [78], [81], [82]. This shape provides the hydrofoil with a high lift-to-drag ratio and high propulsive efficiency [83]. Hydrofoils can be held stationary at various angles of attack or oscillated (Fig. 8; [12], [40], [41], [43], [85]-[87]. The angle of attack is generally a small angle corresponding to the deflection of the hydrofoil from the flow. Lift arises from asymmetries in the flow. The asymmetry generates a pressure difference between the sides of the hydrofoil with a net force normal to the incident flow. Lift is generated continuously with a steady flow. Although some resistive drag is produced by the hydrofoil, it is small compared to the lift. The high lift-to-drag ratio is a function of the high aspect ratio of the hydrofoil [30], [39], [41], [56], [85], [86]. Lift-based appendages to control direction are used by tuna, sharks, sea turtles, penguins, cetaceans, sea lions, and phocid seals.

The performance of the drag-based and lift-based propulsive systems are limited by swimming speed (Fig. 9). Drag-based paddling operates most effectively at low speeds, whereas lift-based hydrofoils perform best at higher speeds. As a flow field needs to be established for a lifting surface to work, hydrofoils are limited in use to conditions where the body of an animal is already in motion. Paddles can be used when the body is stationary. A paddle of large area can impart sufficient momentum to a mass of water to induce a recoil in a stationary body. The reaction force can be used to accelerate the body and produce a maneuver. Because the thrust production by the paddle is dependent on its movement in the direction opposite the body movement, thrust decreases as the velocity of the body increases. At a speed where the body and paddle speeds are equivalent, thrust can no longer be produced [88].

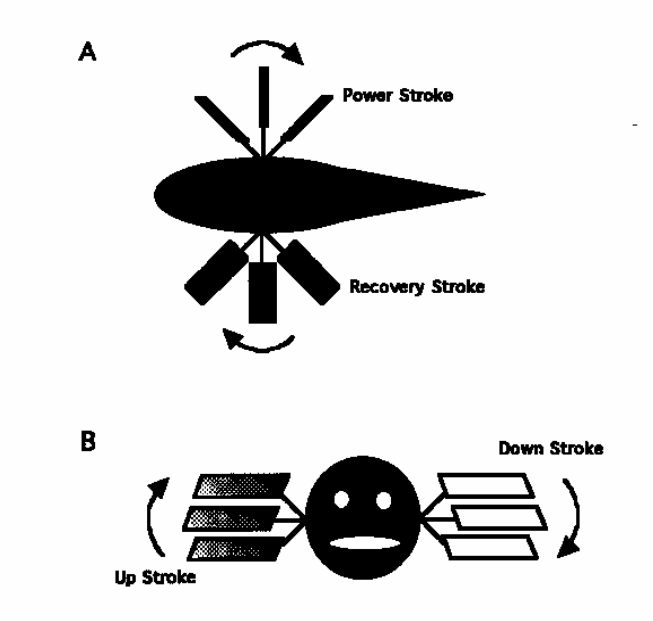

Fig. 8. Simplified motion of drag-based paddle and lift-based hydrofoil. The paddling motions (a) are shown from a top view, the movements of the hydrofoil are shown from a front view. Redrawn from [88].

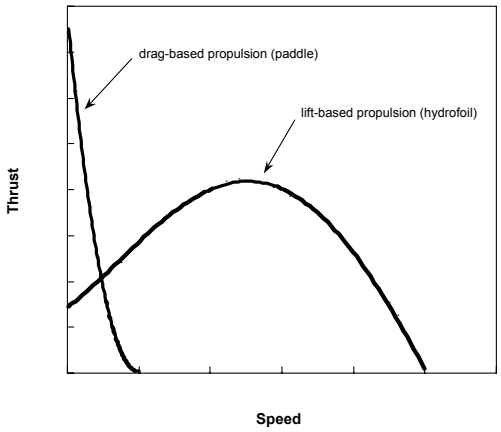

Fig. 9. Comparison of lift-based and drag-based thrust production in relation to swimming speed. Drag-based paddling can result in substantially greater thrust production than lift-based swimming when a body is stationary. As speed increases, drag-based paddling becomes less effective compared to lift-based thrust production. Redrawn from reference [88].

II. LOCATION OF CONTROL SURFACES IN RELATION TO STABILITY

a. Degrees of freedom

Aquatic animals are free to move in three translational (heave, slip, surge) and three rotational (yaw, pitch, roll) directions (Fig. 10). The six different ways of movement are known as the six degrees of freedom [89]. Movement in any of these directions represents an instability. Stability about the roll axis is lateral stability, about the yaw axis is directional stability, and about the pitch axis is longitudinal stability [90]. The position, size and geometry of the control surfaces help to maintain stability and regulate instabilities as required in maneuvering.

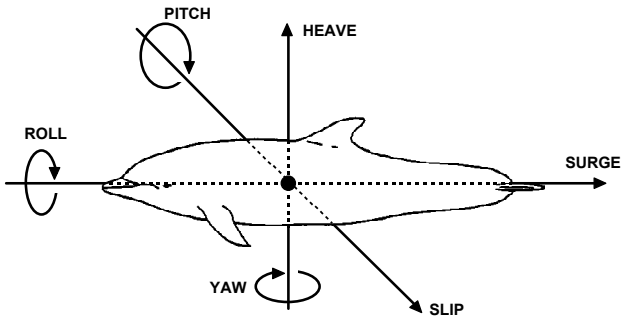

Fig. 10. Translational and rotational instabilities. The position of the center of gravity (CG) is indicated by the solid circle. Rotational and translational instabilities associated with a three-dimensional axis system are projected on the lateral view of the dolphin. Translational instabilities include movement along the three axes as surge (X-axis), heave (Y-axis), and slip (Z-axis). Rotational instabilities include roll (rotation around the X-axis), pitch (rotation around the Y-axis), and yaw (rotation around the Z-axis).

b. Arrow model

To understand how variation in the morphology of animals can affect maneuverability, consideration should be given to parameters associated with stability. Maneuverability represents a controlled instability, and morphological characters that deviate from those of a stable design can be expected to enhance maneuvering performance. Generally, the more stable a body is then the less maneuverable it is [89], [91]. Placement, size, and design of pectoral fins can influence the stability and maneuverability of aquatic animals [62], [81], [91]-[102]. As animals have produced multiple solutions to both stability and maneuverability, the morphological variation expressed by aquatic organisms does not permit any one animal from being a model.

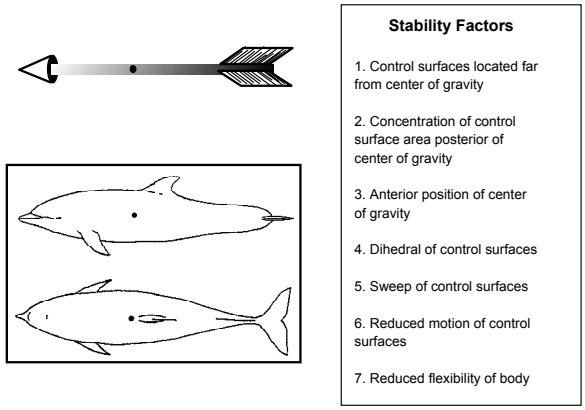

Fig. 11. Comparison of the stable arrow design with the dolphin morphology. Factors associated with stability from an arrow model are listed. The center of gravity on the arrow and dolphin are indicated by the solid dots. From reference [62].

Perhaps the simplest model to use as a standard to assess a stable morphology of an animal moving in a fluid environment is an arrow. An arrow represents a relatively simple technology that is extremely stable for movement through a fluid [103]. Upon being shot from a bow, an arrow becomes self-stabilizing with respect to yaw, pitch and roll. The stabilizing feathers, located at the posterior end of the shaft, produce lift forces to counteract destabilizing turning moments around the center of gravity (CG). In the case of pitch suppression, the sum of aerodynamic forces produces a resultant air force (R), which has an origin at the center of pressure (CP) [103]. As the arrow feathers position CP aft of CG, a torque develops around CG. At angles of attack > 0^o, the torque developed will act to drop the tip of the arrow; whereas, at angles of attack < 0^o, the feathers generate lift in the opposite direction causing a reverse torque that raises the tip of the arrow. The arrow will oscillate for a few cycles before a stable equilibrium is achieved. As the oscillations of the arrow produce the stable flight, this is an example of dynamic equilibrium [103]. Once equilibrium is reached the body is trimmed. Based on analysis of aerodynamics, a number of design features associated with stability are represented in the arrow that can be compared to the morphology of aquatic animals to assess the stability of their design (Fig. 11).

c. Stability parameters

Features associated with placement and design of control surfaces provide stability by producing torques in response to changing flow direction (Fig. 11) [59], [62], [81], [91], [92], [101], [104], [105]. Control surfaces located far from the CG can generate large directionally correcting torques, because of their long lever arm. Propulsors arranged around CG are postulated to promote maneuverability [100]. The relative size of the control surface in relation to its location also will determine the magnitude of the torques [59].

Stable movement occurs with posterior placement of the control surfaces relative to CG [103]. This placement positions the CP aft of CG. The reverse position will create an unstable situation. Perturbations would result in tumbling. Placing the tail fin well aft of CG turns the body into the flow in a manner similar to a weathercock [89].

Both dihedral and sweep of the control surfaces act similarly to stabilize roll and yaw, respectively [56], [91], [92], [106], [107]. Dihedral is a tilting of the control surface relative to the body and sweep is rearward sloping of the leading edge of the control surface. Dihedral is good at resisting side slip and yaw [90]. Because the velocity of a fluid oriented obliquely to the trajectory of the arrow encounters each member of a paired control surface differently, the control surface with a more perpendicular orientation to the flow will generate larger forces than the other control surface and produce stabilizing moments [90]. Rearward sweep results in a backward shift in the center of lift providing increased stability [91]. Alternatively, forward swept control surfaces increase maneuverability [108]. Swept wings can be combined with negative dihedral, also called anhedral, to combat coupled instabilities of yaw and roll [89], although anhedral is considered destabilizing in aerial flight [108]. Reduced motion of the control surface and reduced flexibility of the body restrict self-generated perturbations [101], [102], [109].

The same features that control stability for an arrow are present in the morphology of animals. Unlike the arrow, the animal body is responsible for producing its own propulsive forces. Flexibility of the body and the appendages, by undulation and oscillation, are necessary in the generation of thrust [42], [56], [78]. These propulsive motions produce transverse recoil forces that must be balanced along the body to maintain stability and minimize energy expenditure during locomotion [78], [110]. The increased flexibility for propulsion can produce its own destabilizing perturbations. The various forms of cyclical and symmetrical movements of the body and appendages can act as dynamic stabilizers [87], [111], [112]. When symmetrically applied, the time-averaged propulsive forces maintain an animal on course, although oscillations in the body are apparent. In elongate animals, recoil forces are balanced by multiple body flexures [56], [73]. However, the animal pays a penalty in terms of increased drag [78]. Animals with short or inflexible bodies reduce recoil by changes in the distribution of the projected area in the direction normal to flexure [59], [78].

III. MORPHOLOGY OF CONTROL SURFACES

a. Structural components and mobility

The control surfaces, comprising the hydrofoils (flippers) and paddles of non-piscine vertebrates, are modifications of the limbs of terrestrial animals, which have become adapted for use in water. Both flippers and paddles, therefore, have the same structural elements (i.e., bones) as found in their terrestrial ancestors. Paddles are largely unmodified. Because paddles are used predominately by semi-aquatic animals, they must function for both aquatic and terrestrial locomotion.

Pectoral limbs have a single, proximal humerus, which articulates at the shoulder joint with a broad scapula (Fig. 12; [11], [28], [113]-[116]. In reptiles and birds, the shoulder joint also includes the coracoid. In mammals, the humerus has a ball-and-socket articulation with the scapula. The globular head of the humerus fits into a concavity on the scapula, which is known as the glenoid cavity. Cetaceans also may involve the sternum in the joint cavity [61]. Distally, the humerus articulates with a preaxial radius and a postaxial ulna. The ulna and radius terminate at the wrist joint and articulate distally with a number of carpal bones. The carpals are followed distally by a set of metacarpals and then the phalanges. The phalanges would comprise the digits in terrestrial animals. As in the terrestrial condition, there are five digits with the exception of large whales in the family Balaenopteridae, which lack a thumb [117] and birds, which lost digits in the evolution of the wing for flight. In flippers, the digits are not separated. The number of phalanges in each digit of the flipper is variable between species. Hyperphalangy is the condition in which the maximum number of phalanges exceeds the terrestrial number [11]. Hyperphalangy is found in cetaceans and ichthyosaurs.

The appendicular bones of semi-aquatic and aquatic non-piscine vertebrates differ in proportions from those of terrestrial relatives. Bones of the limbs are robust to accommodate greater muscular and hydrodynamic forces (Fig. 12) [11], [116]. The humerus is short to increase mechanical advantage. The distal bones of paddle-like feet and flippers are elongate [118]. Elongation of the digits increases the surface area of the limb.

Paddle-like limbs of semi-aquatic vertebrates show a similar degree of mobility to those of their terrestrial relatives. Despite the number of bony elements and joints within pectoral flipper, mobility between the joints is constrained in more aquatically derived animals. The flipper is made stiff by layers of fibrous connective tissue. For sea turtles, penguins, seals, and sea lions, there is some flexibility at the elbow, which acts as a hinge joint [114]. In seals and manatees, movement at the elbow occurs when these animals paddle [48], [52]. Otherwise, flexion and extension of the elbow is used primarily during terrestrial locomotion by sea turtles and pinnipeds [8], [52].

Movement of flippers occurs primarily at the shoulder joint. This joint is multiaxial, permitting various movements, including protraction, retraction, adduction, abduction, and rotation [5], [8], [11], [25], [28], [40], [48], [52], [58], [60], [61], [114], [119], [120]. The range of movements at the shoulder varies between taxonomic groups. Animals that use the pectoral appendages to generate propulsive forces display the least limitation in flipper movement. These animals, which include sea turtles, penguins, and pinnipeds, can raise the tips of their forelimbs above the horizontal plane of the body [7], [8], [28], [119]. Penguins can raise their wings to an angle of 45^{o} above the horizontal plane [28]. The use of the flippers for paddling in manatees necessitates a high degree of mobility at the shoulder [48]. Pinnipeds use the flippers for aquatic propulsion, but mobility of the joints in

the flipper also will be associated with the terrestrial locomotion.

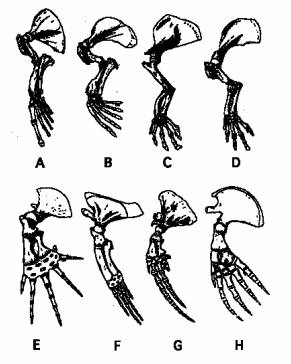

Fig. 12. Skeleton of left pectoral limbs of aquatic mammals including (A) sea lion, (B) seal, (C) manatee, (D) dugong, (E) right whale, (F) blue whale, (G) pilot whale, and (H) river dolphin. From [11] with permission of publisher.

The flippers of cetaceans are positioned on the animal with anhedral (Fig. 11). The flippers generally are constrained in their movements. Reduced motion of the flippers of fast swimming dolphins is necessary to enhance stability [62], [101]. Beaked whales are an exception with small, narrow flippers that can be rotated and adducted to be tucked into slight depressions on the side of the body [121]. This ability may be a mechanism to reduce drag when swimming. Beaked whales are deep (1000m) and long-diving (1 hour) cetaceans and may forgo maneuverability for reduced energy consumption. Humpback whales (*Megaptera novaeangliae*) have long flippers with high mobility. The humpback flipper can be rotated around its long axis by 120^{o} [60]. A tethered whale was able to use the flippers to move the body up, down, forward, backward, and sideways [60].

The mobility of the flippers of fast swimmers appears to be more constrained compared to the flippers of slow-swimming, highly maneuverable animals [11], [60], [61], [101], [122], [123]. The shoulder musculature of *Inia geoffrensis* is highly differentiated in contrast to the faster swimming *Lagenorhynchus*, *Phocoena*, and *Tursiops* [61]. *Inia* is capable of performing a turn with radius that is 10% of its body length [101]. This degree of maneuverability is necessary to operate in the complex environment of a shallow river habitat. Similarly, *Megaptera* uses its long, mobile flippers to maneuver in coastal waters for prey [60], [124], [125].

The amount of muscle within flippers is small. Muscles are confined largely toward the shoulder (Fig. 13). The reduction in muscles distally in the limb are the result of reduced lateral motion of the digits. Semi-aquatic animals with little specialization of the limb have muscles that extend into the digits. Muscles associated with upward (adduction) or downward (abduction) movement of flippers insert on the humerus from the sternum, vertebrae, scapula, and clavicle. The major muscle on the ventral side of the animal is the pectoralis; on the dorsal side, the trapezius and latisimus dorsi. Muscles originating at the scapula can rotate the limb.

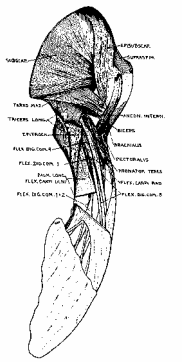

Fig. 13. Musculature of the medial aspect of the left pectoral flipper of a sea lion (*Zalophus californianus*). The bulk of muscle is located proximally in the limb with tendonous and ligamentous connections in the distal part of the flipper. From reference [11] with permission of publisher.

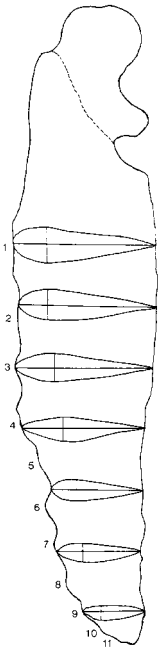

Fig. 14. Flipper planform for *Megaptera novaeangliae*. Flipper planform showing representative cross-sections. Flipper is oriented with its distal tip pointed down. Horizontal lines through each cross-section represent the chord length and vertical lines represent the maximum thickness. Numbers located along the leading edge indicate the center for each of the tubercles. From reference [125].

b. Streamlining and associated hydrodynamic parameters

Planform

Flipper planforms vary from elongate wing-like forms in humpback whale (*Megaptera novaeangliae*; Fig. 14.), sea lions, penguins and sea turtles to rounded paddle-like forms in killer whale (*Orcinus orca*) and beluga (*Delphinapterus*

leucas). The humpback whale has the longest flipper of any cetacean [126] with length varying from 25-33% of body length [60], [127], [128]. The flippers of other cetaceans are no longer than 0.14 body length [60]. For odontocete cetaceans, flipper length directly increases with increasing body length (Fig. 15).

A novel feature on the leading edge of the humpback whale flipper is the presence of 10-11 prominent rounded tubercles (Fig. 14; [125]). The tubercles are large near the body, but decrease in size toward the tip of the flipper. The distance between the tubercles varies from 1.7 to 12.3% of flipper span at the tip and toward the body, respectively. The intertubercular distance is relatively uniform between 6.5 and 8.6% of span over mid-span of the flipper.

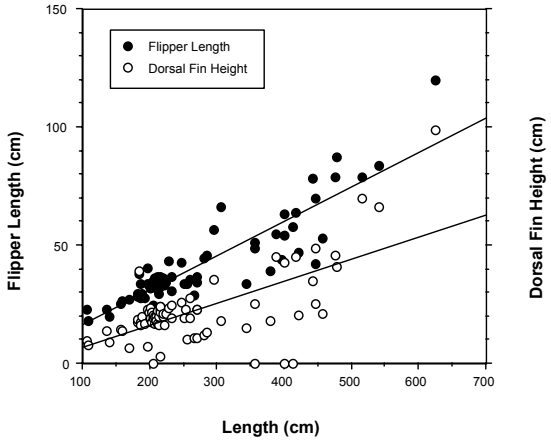

Fig. 15. Relationships between flipper length and dorsal fin height with respect to body length for odontocete whales. A total of 81 individuals were examined from 26 species. Flipper length (*FL*) increased with increasing body length (*BL*) according to the equation $FL = 1.80 + 0.15\ BL$ ($r = 0.89$); dorsal fin height (*DF*) increased directly with *BL* according to the equation $DF = -2.93 + 0.09\ BL$ ($r = 0.65$). From reference [45].

When present in cetaceans, dorsal fins are shaped as falcate, triangular, or rounded [129]. Dorsal fin height is directly related to body length (Fig. 15). The largest dorsal fin (1.8 m high) is found in male killer whales (*Orcinus orca*) and is a distinct sexual dimorphic characteristic in this species. The dorsal fin is typically swept (Fig. 16) with a maximum reported value of 66.2° [45]. No association between swimming speed and dorsal fin design has been found. Finless whales, such as *Lissodelphis*, are considered to be a rapid swimmers [130], whereas the beluga (*Delphinapterus leucas*) is reported to be a slow swimmer [43], [44].

The planform of paddle-like feet of semi-aquatic animals is circular or triangular with the narrowest part of the paddle at the base (Fig. 17). The addition of an interdigital webbing or fringe hairs on the toes increase the surface area of the paddle [11]. During the power phase of the paddling cycle, the toes are spread (abducted) to maximize propulsive surface area. During the recovery phase of the stroke cycle, the toes are pulled together (adducted) and flexed to reduce the area of the paddle. The difference in area of the foot negate a loss of thrust and reduced efficiency between phases within a paddling cycle. Fish [36] reported a 55% reduction in planar area between power and recovery phases of the feet of the muskrat.

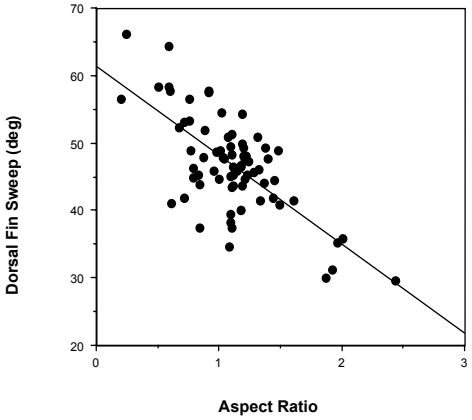

Fig. 16. Relationship of dorsal fin sweep (Λ) to aspect ratio (*AR*) from data in reference [45]. The regression line is described by the equation $\Lambda = 61.29 - 13.16\ AR$ ($r = 0.70$).

The paddle-like foot has a shape that is circular or triangular with a constriction at the attachment point with the body. The constriction minimizes interference drag with the body [131], [132]. In some cases, the constriction displaces the center of area of the paddle further from the body and provides a longer lever arm to increase the velocity of the paddle [36], [74]. Long stroke lengths and high paddling frequencies are not efficient; it is more efficient to generate thrust by acceleration of a large fluid mass to a small velocity than a small mass to a high velocity [72]. In small semi-aquatic rodents with high paddling frequencies and small paddle areas, inertial and added mass effects account for 31-51% of the total energy necessary for paddling [42]. When paddles are used for maneuvering, however, efficient force production may not be necessary. Maneuvering in animals typically requires the rapid production of destabilizing forces without considerations of efficiency or economy.

Tests on models of fish demonstrated that fins with circular and triangular planforms produced greater pressure drags than square or rectangular planforms [132]. A triangular fin shape has a greater moment of inertia than square and rectangular fins [132]. Paddles with a triangular shape can generate thrust while reducing energy losses due to added mass and inertial effects. When swept through an arc, the distal segment of the paddle produces the majority of the thrust, because it experiences the highest flow rate. Blake [74] found that 80% of the thrust and work produced was produced by the distal quarter of a triangular fin.

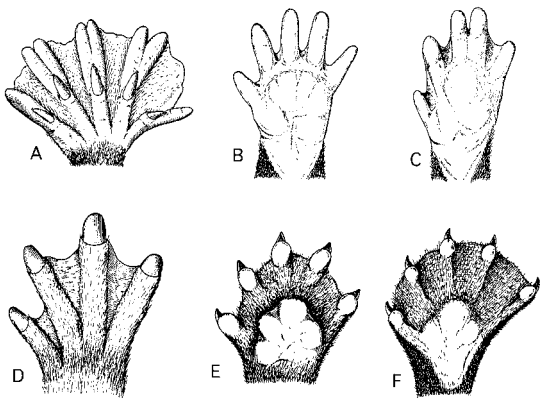

Fig. 17. Anterior feet of semi-aquatic mammals showing the range of interdigital webbing, which is used as a paddle. (A) platypus, (B) African clawless otter, (C) oriental small-clawed otter, (D) capybara, (E) North American river otter, and (F) spotted-necked otter. From reference [11] with permission of publisher.

Aspect ratio

The aspect ratio, AR, of biological control surfaces is calculated as the square of the span divided by the planar area [56]. In cetaceans, the *AR* of flippers is most pronounced for the humpback whale, *Megaptera* (*AR*=6.1; [125]). For odontocete flippers, *AR* values range from 1.9 for paddle-like flipper of *Orcinus orca* to 7.7 for the highly swept, elongate flipper of *Globicephala melaena* [45]. Dorsal fin *AR* is significantly smaller than the flipper *AR*. The largest dorsal fin *AR* of 2.4 is found for a male *Orcinus orca*. For cetaceans that possess a dorsal fin, the smallest *AR* is displayed for the triangular fin of *Inia geoffrensis*. Dorsal fin sweep is inversely related to *AR* (Fig. 16) so that animals with high sweep have low *AR* and *vice versa*.

AR for penguin flippers varies from 4.2 to 4.5 [29]. Fish et al. [133] reported *AR* for two sea lions as 4.1 and 4.2. However, Feldkamp [39] reported an average *AR* of 7.9 for sea lion flippers, when *AR* was calculated as span of the flippers divided by their chord.

Cross-sectional design

Cross-section design of flippers and other control surfaces displays the characteristic fusiform design (Fig. 18; [29], [40], [113], [125], [134], [135]. Due to the addition of skeletal elements in the flippers, these appendages are relatively thick compared to control surfaces that are composed solely of collagenous material, such as the flukes and dorsal fin of cetaceans. Flippers of penguins are cambered in cross-section [29], whereas, flippers of marine mammals, such as sea lions and cetaceans, are uncambered (i.e., symmetrical about the chord line) [40], [125]. The tip of the humpback whale flipper is scooped out along the ventral surface of the leading edge, producing a concavity [125], [127].

Despite the similarity of cross-sectional designs of flippers with engineered foil sections, flippers have not been fully analyzed with the rigor demonstrated for wing sections. Available data on sectional characteristics of high aspect ratio control surfaces from marine mammals and penguins are provided in Table 1. The most typical index of shape used to describe the cross-sectional geometry of flippers is the maximum thickness as a percent of chord length (inverse of fineness ratio). At mid-span, biological control surfaces have thicknesses ranging from 15.0 to 24.0% of chord (Table 1). Maximum thickness varies along the span of flippers with lower values closer to the root. For penguins, the maximum thickness as a percent of chord length varies from 14 to 17% [29]. Sectional thickness of the sea lion (*Zalophus californianus*) flipper varies from 31.3% of chord at the root to 18.5% of chord near the tip [40]. Conversely, humpback whale flippers have high sectional thickness at the tip (27.8% of chord) with the lowest sectional thickness (20% of chord) near mid-span [125].

Table 1. Sectional characteristics from mid-spans of control surface fins from cetaceans, sea lions and penguins. Data from[29], [39], [125], [134], [179], [180].

Species	Fin type	Maximum thickness % chord	Distance from leading edge to maximum thickness % chord	Leading edge radius % chord	Trailing edge thickness % chord	Distance from leading edge to maximum camber % chord	Minimum Cp	Distance from leading edge to minimum Cp % chord
Delphinus bairdi	fluke	21.1	32	4.2	0.46	symmetrical	-0.74	15
Lagenorhynchus obliquidens	fin	19.3	33	3.8	0.90	symmetrical	-0.66	14
Phocoenodies dalli	fin	15.2	36	2.4	0.28	symmetrical	-0.46	16
Megaptera novaeangliae	flipper	20.0	33			symmetrical		
dolphins	fluke	19.0-24.0	24.0-30.0	3.2-7.4		symmetrical		
Zalophus californianus	flipper	21.3	24.4			symmetrical		
Pygoscelis antarctica	flipper	15.0	35	3.0		30		
Pygoscelis adeliae	flipper	15.0	30	4.0		50		
Pygoscelis papua	flipper	15.5	30	2.5		50		

The distance from the leading edge of the high *AR* control surface to the maximum thickness varies 24 to 36% of chord (Table 1). The placement of the maximum thickness indicates a fairly even pressure distribution in the chordwise direction [134]. This morphology would potentially delay separation. In addition, the prominent leading edge radius would prevent leading edge separation during maneuvers with increased angle of attack.

Camber in penguin flippers effectively increases lift production. While camber may be a remnant of an evolutionary pathway from flight, the wing structure can be useful in force production for propulsion and turning maneuvers.

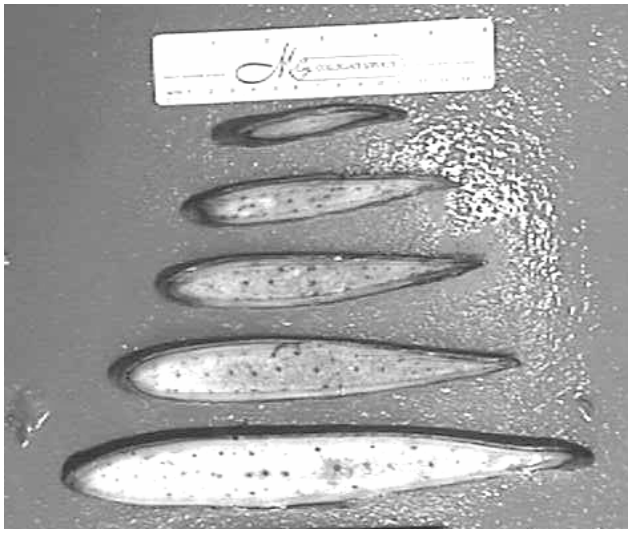

Fig. 18. Sections of dorsal fin from bottlenose dolphin (*Tursiops truncatus*). From reference [45].

Lift and drag characteristics

Well-designed control surfaces maximize the ratio of lift (L) to drag (D) generated by their action or passive from the ambient water flow [56], [98]. An increase in the maximum L/D with increasing size is achieved by increasing span of the control surface more rapidly than the square-root of planar area, thereby increasing *AR* [82], [136], [137]. The longer span of a high *AR* fluke increases the mass of water deflected posteriorly, augmenting lift. However, *AR* above 8-10 provides little further advantage [56], [113].

The addition of appendages increases the drag. As the pectoral flippers of sea turtles, penguins, and sea lions are used for propulsion, it is impossible to differentiate the thrust from the drag for these appendages and drag estimates have not been performed. Many cetaceans, however, have flippers that project laterally from the body and add substantially to the total drag. The body of the harbor porpoise (*Phocoena phocoena*) makes a disproportionate contribution to the total drag in that the body is 87.6% of the total surface area, but only 64.3% of the drag [138]. The dorsal fin, pectoral flippers, and flukes comprised only 2.6, 4.2, and 5.6% of the total surface area of the harbor porpoise, respectively; however, these appendages are responsible for 35.7% of the total drag (4.3, 18.0, 13.4 %, respectively). The drag added by the appendages of *Tursiops* was estimated as 28% of the total drag [139]. The added increase in drag due to the appendages is caused by interference drag as flow over the body is distorted by the appendages and induced drag from differential pressure in lift generation by the appendages [30], [44], [56], [88], [131]. The induced drag component is the energy lost due to tip vortices that are generated by pressure differences between the two sides of the flippers and dorsal fin during maneuvers [30], [56].

The induced drag is highly dependent on *AR*, with high drag associated with low *AR*, untapered hydrofoils [56]. Induced drag is produced as a consequence of the lift generated by the control surface. When canted at an angle to the water flow, lift is produced by deflection of the water and pressure difference between the dorsal and ventral surfaces of the control surface [43], [56], [73], [86]. The pressure difference produces spanwise cross flows that go around the control surface tip resulting in the formation of spiraling vortical flow. The flow is shed from the fluke tip as longitudinal tip vortices. The energy dissipated by the vortices represents the induced drag. High *AR* and tapering of the flippers reduces tip vorticity and induced drag [24], [56], [71].

Induced drag also is limited by the sweep. van Dam [82] showed that a tapered wing with sweepback or crescent design could reduce the induced drag by 8.8% compared to a wing with an elliptical planform. Minimal induced drag is fostered by a swept wing planform with a root chord greater than the chord at the tips, giving a triangular shape [140], [141]. This optimal shape approximates the planform of flippers [29], [45].

Sweep together with taper has the effect of concentrating the surface area toward the trailing edge. This would effectively shift the lift distribution posterior of the center of gravity, affecting pitching equilibrium [56], [136]. The combination of low sweep with high *AR* (Fig. 16) can aid in lift generation for maneuvers. Highly swept-back, low *AR* wings produce maximum lift when operating at large angles of attack, when low sweep, high *AR* designs would fail [107]. However, the maximum lift is reduced with increasing sweep angle for a given *AR* [142]. The relationship between sweep and *AR* also indicates a structural limitation to the strength and stiffness of the control surfaces [82], [143]. The ability to sustain certain loads without breaking is considered a major constraint on increasing span and *AR* [144].

Analysis of the pressure distribution of non-mobile control surfaces in dolphins was performed by Lang [134]. Using a two-dimensional, potential flow, airfoil program, he calculated the pressure distribution for single sections from the dorsal fins of the Pacific striped dolphin (*Lagenorhynchus obliquidens*) and Dall's porpoise (*Phocoenoides dalli*). Their minimum pressures were located 14-16% of chord (Table 1; Fig. 19), followed by a region of gentle adverse pressure gradient to 50-60% of chord, and followed by a steep adverse pressure gradient (Fig. 19). Lang [134] considered that the fins were ideally suited to operate at a Reynolds number of 10^6. The fins normally operate at this Reynolds number.

The fin sections examined by Lang [134] were considered relatively thick at 19.3 and 15.2% of chord for *Lagenorhynchus* and *Phocoenoides*, respectively. This thickness may add to the strength of the fin and may permit greater variations in angle of attack during maneuvers. The section geometry could prevent excessive minimum pressure peaks at the leading edge, and thus prevent flow separation and cavitation. Cavitation near the water surface was expected to occur with a zero angle of attack of 17.3-20.7 m/s [134].

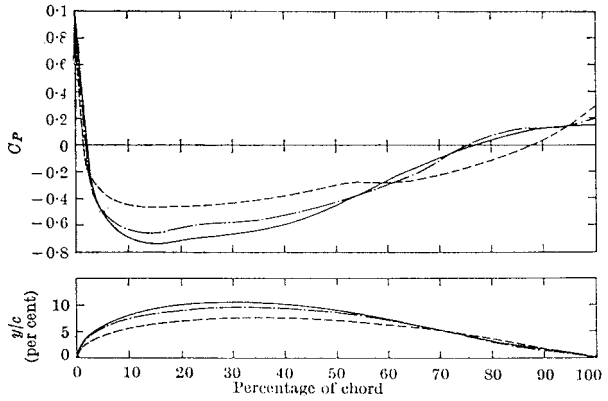

Fig. 19. Profiles (lower) and pressure distribution (upper) for sections at 50% of span for the tail fluke of the common dolphin, *Delphinus bairdi* (——), dorsal fin of the Pacific striped dolphin, *Lagenorhynchus obliquidens* (_ . _ . _) and dorsal fin of Dall's porpoise, *Phocoenoides dalli* (- - - -). From reference [134] with permission of author and publisher.

Pressure distributions of the fins and flukes from dolphins (Fig. 19, E.20) were not considered similar to common airfoils [134]. Fin profiles were judged to be a compromise between airfoils FX05-191 and EA6(-1-)-018. The favorable pressure gradient near the nose and gentle adverse gradient appeared to optimize the length of the laminar boundary layer and resist separation [134]. At angles of attack up to 4°, the dolphin fin should not incur separation and increased drag (Fig. 20).

When actively swimming, bioluminescent "contrails" frequently have been reported [145]-[147] extending from the flukes, flippers, and dorsal fins of dolphins. These contrails are the tip vortices generated from the differential pressures along the two surfaces of a lifting surface.

Flow visualization using bioluminescence within the boundary layer of a dolphin was exploited by Rohr and Latz with their colleagues [148], [149]. The bioluminescence is produced by unicellular plankton called dinoflagellates. The bioluminescence response of the dinoflagellates was calibrated to a hydrodynamic induced shear stress [148]. Stimulation of bioluminescence occurred above a shear stress of approximately 1 dynes/cm^2 in both laminar and turbulent flows. A gliding dolphin moving through water with the dinoflagellates was able to stimulate bioluminescence over its body (Fig. 21; [149]). There was a conspicuous lack of bioluminescence over the leading edges of the flippers and dorsal fin. During rectilinear glides, the boundary layer remained attached over the surface of the dorsal fin and flippers. Flow separation was noted at the trailing edges of these control surfaces. From Fig. 21, disturbed flow can be observed at the base of the flippers potentially due to interference effects. Lines of bioluminescence were apparent from the tips of the dorsal fin and flippers when the dolphin executed a turning maneuver [149]. These contrails were most likely the result of pressure differences between the sides of the control surfaces, which were associated with lift generation.

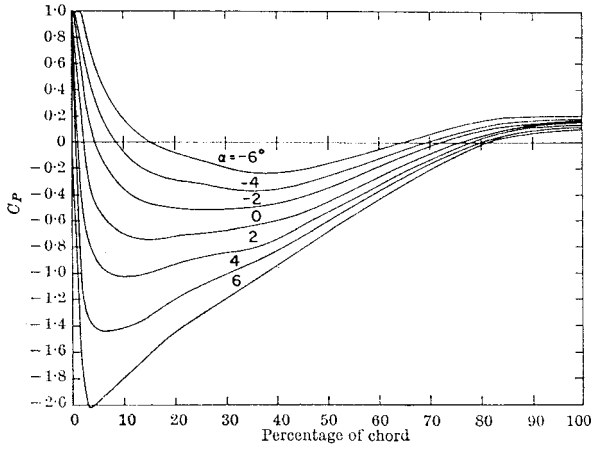

Fig. 20. Effect of angle of attack on the pressure distribution of a two-dimensional foil based on a section from a dolphin fluke at 50% of span. From reference [134] with permission of author and publisher.

The position and number of tubercles on the humpback flipper suggest analogues with specialized leading edge control devices associated with improvements in hydrodynamic performance. Bushnell and Moore [150] suggested that humpback tubercles may reduce drag on the flipper. The occurrence of "morphological complexities" on a hydroplane could reduce, or use, tip bleed flow to decrease drag and improve lift generation to prevent tip stall. Alternatively, various biological wings utilize leading edge control devices to maintain lift and avoid stall at high attack angles and low speeds [151]. Hydroplanes used in turning must operate at high angles of attack while maintaining lift.

Fish and Battle [125] considered that the tubercles of the humpback whale flipper may function to generate vortices by unsteady excitation of flow to maintain lift and prevent stall at high angles of attack. The function of the tubercles would be analogous to strakes used on aircraft. Strakes generate large vortices that change the stall characteristics of a wing [125], [131], [152], [153]. Stall is postponed because the vortices exchange momentum within the boundary layer to keep it attached over the wing surface. Lift is maintained at higher angles of attack with strakes compared to wings without strakes, although maximum lift is not increased by strakes. Increased angle of attack is necessary during turning maneuvers to generate the lift force for the turn [91], [107], [136]. The ability to maintain lift at high angles of attack would be advantageous for humpback whales in maneuvering.

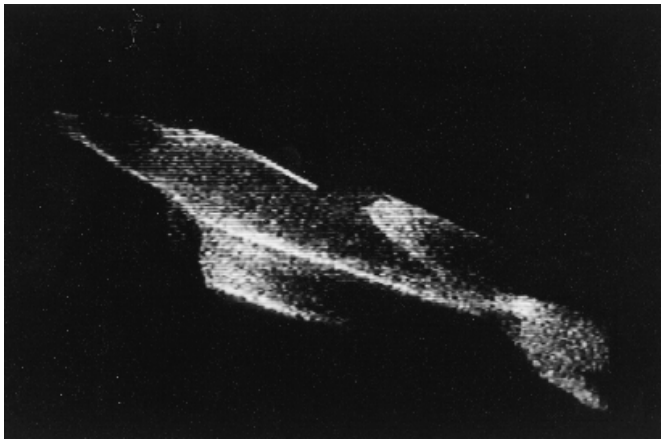

Fig. 21. Bioluminescence image of a gliding dolphin (*Tursiops truncatus*). From reference [149] with permission of author.

Flow visualization experiments conducted on a model wing section with leading edge tubercles similar to those on humpback flippers showed that vorticity was produced (Wallace and Smith, personal communication). Bearman and Owen [154] demonstrated that a wavy leading edge on a bluff body produced a 30% drag reduction. The wavy leading edge generates periodic variation in the von Karman wake across the span [155]. A wide wake occurs at a trough (i.e., leading edge loops downstream) and a narrow wake occurs at a peak in the leading edge. An inviscid panel method simulation of a NACA 63_4-021 wing with leading edge tubercles showed a 4.8% increase in lift and a 10.9% reduction in induced drag at 10^o angle of attack [153].

IV. Maneuvering performance

a. Cetacean maneuvering

In general, cetaceans possess a morphological design similar to that found in the arrow model (i.e., anterior position of CG, concentration of control surfaces posterior of CG, dihedral and sweep of control surfaces) that enhances stability, thereby potentially constraining turning performance [62]. Compared to fishes, cetaceans have few control surfaces.

The flippers of cetaceans act to passively dampen the rate of growth of a perturbation [59]. The position of the flippers increases both the area and span of the body anterior of the center of mass. Pitching movements will produce a force normal to the planar area of the flippers that will act to resist vertical motions of the head. The increased area of the flippers increases the added mass and inertia at the anterior end of the animal effectively dampening recoil movements [56], [110]. The vertical movements of the flippers are asynchronous with the propulsive cycle of the flukes [87]. The large phase differences between the motions of the flippers and the flukes of cetaceans help to generate resistive forces at the flippers that would counter pitching rotations generated by the vertical forces produced by the flukes. However, cetaceans with flippers of relatively large areas showed no effect with respect to decreasing dorso-ventral excursions at the rostrum [87]. One possible reason for this observations is that cetaceans do not show differences between the planar area of the flippers and the planar area of the flukes. Since fluke area is proportional to force production, the resistive force generated from recoil at the flippers would be proportionally similar.

A dimensionless maneuverability index was used by Maslov [63] to compare the turning performance of dolphins with submarines. The index was a compilation of variables including length, mass, turning velocity, time to execute the turn, power output, and turning radius. The results of the comparison showed that dolphins were more maneuverable than submarines (USS Albacore, USS Skipjack). Length-specific turning radii for a common dolphin and bottlenose dolphin ranged from 0.5 to 1 *L*. Maslov [63] and Aleyev [59] considered that dolphins turned most effectively around the pitch axis, because of the orientation of the flippers and flukes. Within the horizontal plane, dolphins were considered more stable.

Fish [62], [101] examined the horizontal turning performance of various cetaceans, including the bottlenose dolphin (*Tursiops truncatus*), killer whale (*Orcinus orca*), Commerson's dolphin (*Cephalorhynchus commersonii*), Pacific white-sided dolphin (*Lagenorhynchus obliquidens*), false killer whale (*Pseudorca crassidens*), beluga (*Delphinapterus leucas*), and Amazon river dolphin (*Inia geoffrensis*). *Orcinus* was the largest cetacean with one individual of 4536 kg; whereas the smallest at 29 kg was *Cephalorhynchus*. *Pseudorca* and *Lagenorhynchus* were regarded generally as fast swimmers; whereas, *Delphinapterus* and *Inia* are considered to be slow swimmers [45]. *Delphinapterus* and *Inia* are different from the other cetaceans by possessing mobile necks and flippers. *Inia* is capable of a notable degree of lateral flexion. In addition, the dorsal fin is reduced in *Inia* and absent in *Delphinapterus*.

Cetaceans, executing yawing turns showed two turning patterns: powered and unpowered [62], [101]. Powered turns were defined as turns in which the animal was continuously propelling itself by the dorso-ventral oscillations of the flukes; whereas in unpowered turns, the animal glided through the turn without apparent use of the caudal propulsor. Turns were initiated from the anterior of the animal with lateral flexion of the head and rotation of the flippers into the turn. The flippers also were adducted. During unpowered turns, substantial lateral flexion of the peduncle was observed in addition to twisting at the base of the flukes. At the beginning of a turn, *Tursiops* will twist the inside fluke blade downward by15-45^o from the horizontal, before reversing the rotation of the flukes by 58-88^o as the animal exits the turn [62]. *Pseudorca* flexes its body during the turn and only twists its flukes at the end of the turn by 18-53^o with the outside fluke blade depressed. The twisting action allows the animal to use the flukes in conjunction with the peduncle as a rudder. This action is only possible in unpowered turns because the control surfaces are uncoupled from propulsion, permitting increased flexibility of the spine [62]. Inward banking occurs during unpowered turns.

Rolling oscillations around the longitudinal axis occurred during powered turns that were associated with propulsive fluke motions.

Both *Inia* and *Delphinapterus* proved to be exceptions to the general cetacean turning pattern [62], [101]. *Inia* showed no tendency to bank during turns. *Inia* used its flexible body to produce the turn. Without a dorsal fin, *Delphinapterus* would bank 90^{o} with its ventral surface facing into the turn. This action allowed *Delphinapterus* to use a greater surface area and provided greater body flexion to effect the turn. High bank angles also are displayed by penguins and sea lions, that lack a dorsal fin [46], [156].

The force necessary to maintain a curved trajectory of a given radius is directly related to the square of the velocity and the mass of the body [157], [158]. Minimum turning radius plotted for cetaceans was associated with body mass (Fig. 22). Unpowered turns for cetaceans had smaller minimum radii than powered turns for the same individuals [62]. Cetaceans generally demonstrated minimum unpowered turning radii of < 0.5 *L* (Fig. 22). Minimum radii within each species ranged from 0.11 to 0.17 *L*. A 5 m long *Orcinus* was able to turn within 0.4 *L* [101]. The turn was performed by depressing the posterior half of the body and rotating around the vertically oriented tail. Although the turning radius was small, the speed was low (0.93 m/s) due to the extra drag produced from the body orientation.

Different levels of performance between species were indicated when all the data for turning radius were plotted as a function of velocity (Fig. 23). *Inia* and *Delphinapterus* produced low-speed, small radius turns. Faster speed but larger radius turns were performed by *Lagenorhynchus* and *Cephalorhynchus* and intermediate performance was displayed by *Orcinus*, *Pseudorca* and *Tursiops*.

Turning rate performance is illustrated in Fig. 24 by a plot of centripetal acceleration and turning rate. Most data for cetaceans is clustered at accelerations < 1.5 *g* with turning rates < 200 deg/s. Individuals of *Cephalorhynchus, Lagenorhynchus,* and *Tursiops* were able to exceed these lower values for cetaceans with *Lagenorhynchus* displaying the maximum performance with an acceleration of 3.6 *g* and turning rate of 453 deg/s during unpowered turns. Other cetaceans exhibited generally lower performance. The lowest centripetal accelerations occurred in *Inia* followed by *Delphinapterus* which both swam slowly during testing. Although higher than underwater vehicles (Fig. 25; [63], [104], [105], turning rates were lower than exhibited by fish, penguins, and sea lions [95], [101], [104], [105], [156], [159].

Flexible bodies and mobile control surfaces provide mechanisms to induce instabilities for turning maneuvers. Cetaceans with more flexible body designs (e.g., *Inia*, *Delphinapterus*) sacrifice speed for maneuverability, whereas species with more restricted flexibility (e.g., *Lagenorhynchus*, *Cephalorhynchus*) produce faster but wider turns [101], [160]. As morphological differences can be correlated with behavioral differences [161], features that affect stability and maneuverability of cetaceans appear to be associated with their prey type and habitats.

Inia inhabits rivers, lakes, and floodplain forests and grasslands. Theses habitats are structurally complex, where decreased turn radius and precise, slow maneuverability would be necessary. Similarly, the distribution of *Delphinapterus* is in complex environments including shallow waters, coastal habitats, rivers, and pack ice. *Delphinapterus* feeds on less mobile prey such as bottom organisms and large zooplankton [160]. The more stable design of fast swimming cetaceans may limit these animals to locomoting and foraging in pelagic habitats.

The ability to roll permits cetaceans to reorient their body to take advantage of the increased flexibility by ventral flexing of the bodies. Aerial views of foraging dolphins (*Tursiops truncatus*) showed that the animals rolled 90^{o} during the final lunge for fish [162]. Bending of the body allowed the tip of the rostrum to turn at a rate of up to 1370 deg/s with a radius of 0.08 body lengths.

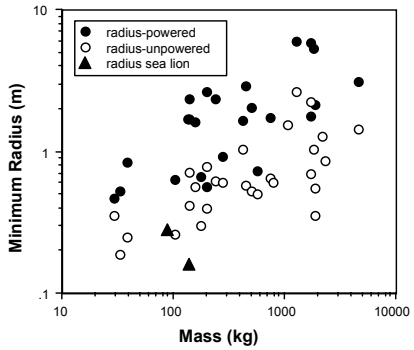

Fig. 22. Minimum turning radius plotted against body mass for individuals from Fish [101]. Circles represent cetaceans for powered (solid) and unpowered (open) turns and triangles represent unpowered turns by sea lions (*Zalophus californianus*).

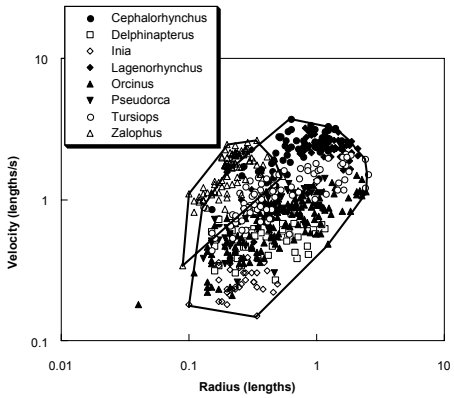

Fig. 23. Average length-specific velocity in relation to length-specific turning radius. Polygons are drawn around data for cetaceans and around data for *Zalophus*. The single point outside the cetacean polygon represents a 1725.2 kg, 5.05 m *Orcinus* which was able to produce a turn radius of 4 % of body length by ventrally flexing the posterior half of the body The flukes were used to pivot the animal around its longitudinal axis.

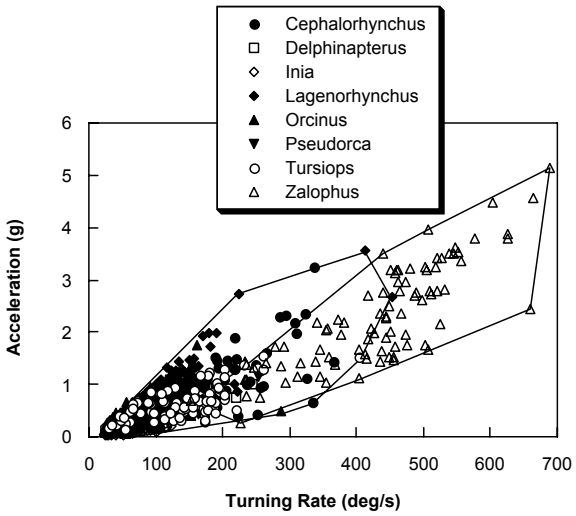

Fig. 24. Relationship between centripetal acceleration and turning rate. Polygons are drawn around data for cetaceans and around data for *Zalophus*.

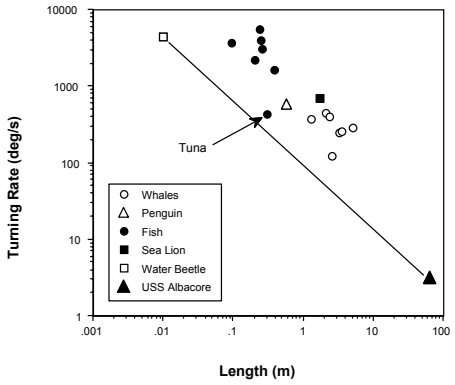

Fig. 25. Turning rate as a function of body length. Data from [95], [101], [156], [163]-[165].

A remarkable maneuver undertaken by spinner dolphins (*Stenella longirostris*) is to leap out of the water and rapidly spin around its longitudinal axis [166]. Although the preparatory movements prior to the leap have not been observed, the dolphin has to start spinning before it leaves the water. Underwater video of Pacific striped dolphins (*Lagenorhynchus obliquidens*) spinning while swimming horizontally shows that the dolphin spins by using its flippers to provide the force to rotate its body (pers. obs.).

b. Sea lion maneuvering

Compared to cetaceans, the placement of control surfaces, mechanisms of propulsion and body configuration indicate greater instability and thus maneuverability by California sea lions (*Zalophus californianus*). The control surfaces of *Zalophus* are represented by pectoral and pelvic flippers [46], [119]. The roots of the larger pectoral flippers are located near CG [101]. This placement of the pectoral flippers is dynamically unstable. The flippers provide little rotational dampening about the yaw and pitch axes (Fig. 26), although they could retard rotational and translational motion in regard to roll and heave, respectively. The smaller pelvic flippers are in the preferred location to develop sufficient torque to act like an airplane stabilizer or ship rudder, and resist rotational instabilities (Fig. 26).

The attitude of the *Zalophus* control surfaces are highly variable because of the high mobility of the pectoral and pelvic flippers [46], [119]. Both the sweep and the dihedral can be changed. The ability of the sea lion to adduct the pectoral flippers against the body and adduct the pelvic flippers can effectively produce a condition where the animal is devoid of control surfaces and potentially susceptible to all instabilities. The mobility of the pectoral and pelvic flippers also permits dynamic production of lift that can induce torques around CG to promote instabilities. The location of the pectoral flippers close to CG would not produce large torques and would be less effective in rapidly inducing turns. The large projected area of the flippers may help compensate for the reduced torque. However, the pectoral flippers are used for propulsion [11], [39], [40], and propulsors arranged around CG are postulated to promote maneuverability [100].

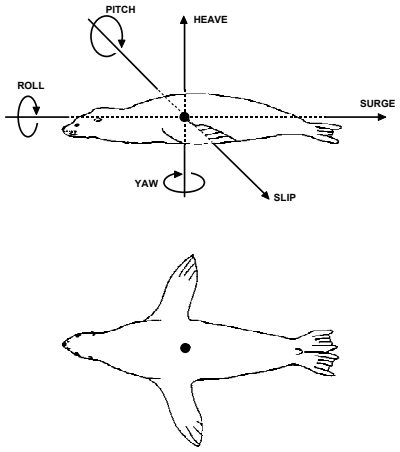

Fig. 26. Illustrations of the flipper design and location for the sea lion from lateral (top) and dorsal (bottom) views. The position of the center of gravity (CG) is indicated by the solid circle. Rotational and translational instabilities associated with a three-dimensional axis system are projected on the lateral view of the sea lion. Rotational instabilities include roll (rotation around the X-axis), pitch (rotation around the Y-axis), and yaw (rotation around the Z-axis). Translational instabilities include movement along the three axes as surge (X-axis), heave (Y-axis), and slip (Z-axis).

The body of *Zalophus* is highly flexible (Fig. 27). Bending of the body and neck is an integral component of turning in conjunction with the flippers of pinnipeds [46], [59]. The

extremely pliable neck and body permit a sea lion to bend over backwards reaching its pelvic flippers [167]. This dorsal bending was the preferred bending direction used by sea lions during turns [46]. Dorsal bending of the spine allows the body to curve smoothly, maintaining a streamlined appearance throughout a turn. As the turn is unpowered, a streamlined body will minimize drag and limit deceleration as direction changes.

Sea lions use only unpowered turns [101]. As described [46], [53], [101], [119], [168], the anterior end of the animal initiates the turn as the sea lion rolls 90^{o} so that the ventral (abdominal) surface faces the outside of the turn and the body is flexed dorsally. The fore- and hind flippers are abducted and held in the vertical plane. This maneuver brings the full area of the flippers into use. In addition, the position of the foreflippers is set to execute a power stroke and accelerate the sea lion as it comes out of the turn.

Fig. 27. Demonstration of body flexibility by the California sea lion.

Sea lions were able to make small radius turns while at high speed (up to 4.5 m/s). Minimum unpowered turn radii for *Zalophus* ranged from 0.9 to 0.16 *L* [101]. While the length-specific radii were small, they were not substantially different from similar values for cetaceans (Fig. 22). However, *Zalophus* typically demonstrated smaller turn radii at higher speeds than cetaceans (Fig. 23). In addition, turning rates were higher for *Zalophus* exceeding the maximal performance of cetaceans (Fig. 32). Sea lions are able to execute turns of 5.13 *g* turn at 690 deg/s. This performance exceeds the acceleration experienced during lift-off on a space shuttle [101].

Similarities have been made between the turning maneuvers of sea lions and the banking turns displayed by birds and airplanes [53]. In these latter banking turns, the wings generate lift that is resolved into vertical and horizontal vector components. The vertical component counters the gravitational force and keeps the aircraft from losing altitude. The horizontal vector is directed toward the center of rotation and provides the centripetal force necessary for the turn.

As sea lions swim in an environment with a density similar to their body composition, these animals can be near neutrally buoyant, negating the necessity of a vertical component during turns in the horizontal plane. Thus, the sea lion can bank 90^{o} without changing depth. The horizontally directed lift from the flippers would produce centripetal force necessary for the turning maneuver. While the pectoral flippers can be rotated to produce an angle of attack (i.e., angle between the flipper chord and the incident flow), bending of the spine would aid in orientation of the flippers for lift generation. However, there is no direct evidence that the flippers are canted at an angle of attack to effect a turn. Indeed, the location of the flippers close to CG reduces the torque to produce the turn. The pectoral flippers are particularly important in generating lift necessary to roll the body. Other surfaces used to control the turn are the head and pelvic flippers. The head leads the turn and determines direction. The pelvic flippers act as stabilizers to prevent the posterior portion of the body from deviating from the curved trajectory of the turn [46].

c. Humpback whale maneuvering

The humpback whale (*Megaptera novaeangliae*) is the most acrobatic of the baleen whales. Its elongate wing-like flippers are important in its ability to maneuver. Observations of swimming performance by humpback whales show them to be highly maneuverable [127], [169], using their extremely mobile flippers for banking and turning [60], [170]. This maneuverability is associated particularly with the feeding behavior of humpback whales. These whales feed on patches of plankton or fish schools including euphausiids, herring, and capelin [124], [171], [172]. Turning is widely used in feeding employed with lunging and bubbling behaviors [173].

In lunge feeding, whales rush (approximately 2.6 m/s) toward their prey from below while swimming up to the water surface at a 30^{o}-90^{o} angle [124], [173]. In "inside loop" behavior, the whale swims away rapidly from the prey aggregate with its flippers abducted and protracted [60], then rolls 180^{o} making a sharp U-turn ("inside loop"), and lunges toward the prey [173]. The entire "inside loop" maneuver is executed in 1.5-2 body lengths of the whale. Rapid turning maneuvers are required also for "flick feeding", which is performed in approximately 3 s [124]. In this feeding behavior, the whale dives until the base of the flukes is at the water surface and the tail is flicked forward, producing a wave. The whale surfaces with its mouth open into the wave.

In "bubbling" behaviors, underwater exhalations from the blowhole produce bubble clouds or columns which concentrate the prey [171], [174]. Columns of bubbles arranged as rows, semicircles, and complete circles form "bubble nets" [124], [173]. Bubble nets are produced as the whale swims toward the surface in a circular pattern from a depth of 3-5 m. At completion of the bubble net, the whale pivots with its flippers and then banks to the inside as it turns sharply into and through the center of the net [173], [175].

Bubble net size varies from a minimum diameter of 1.5 m for corralling euphausiids to a maximum diameter of 50 m to capture herring [124].

Fish and Battle [125] computed the turning radius for a 9 m humpback whale. Their computations were based on the whale using the pectoral flippers to generate a centripetal force for the turn. The whale's minimum turning radius equaled 7.4 m when the banking angle (ϕ) equaled 90^{o} (Fig. 28). The calculated minimum turning radius fell within the minimum and maximum radii for turns during bubbling behaviors [124]. Maximum bubble net radius (25 m) may be achieved by the humpback whale with a banking angle of 17^{o}. Considering that other surfaces of the whale (e.g., flukes, peduncle, body) are employed in turns [60], the actual minimum turning radius was assumed to be smaller [125]. Fluke span is 27-38% of total body length [126], [127]. The relatively large size of the flukes would contribute to maneuverability by increasing the lift force. However, the restricted range of motion of the flukes and body in conjunction with their use in thrust production limits their effectiveness to control maneuverability during powered swimming.

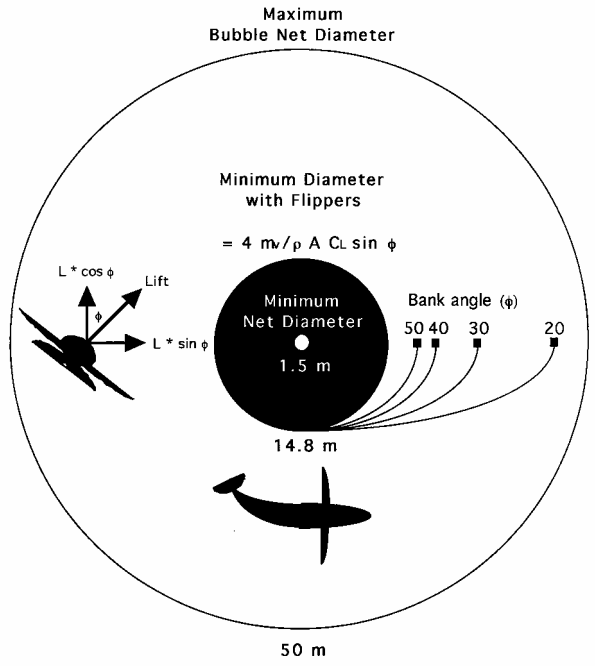

Fig. 28. Calculated and observed turning performance of the humpback whale (*Megaptera novaeangliae*). The calculated minimum turning diameter (14.8 m) for a 9 m whale is shown by the outer margin of the black circle, based on the equation shown. The margins of the turn for various bank angles are shown by curved lines. The minimum and maximum diameters of bubble nets are shown by the margin of the central white circle and the outer white circle, respectively. The lift (L) vectors with respect to bank angle are illustrated in the inset. The silhouette indicates the dimensions of the whale.

d. Penguin maneuvering

Hui [156] examined the maneuvering performance of swimming Humboldt penguins (*Spheniscus humboldti*). He observed that the birds used a variety of body structures to produce turns. The steering structures included laterally compressed tail and hind feet (100% of turns analyzed), laterally compressed beak (95% of turns analyzed), and wings (35% of turns analyzed). Wings were used when maximum power for the turn was required. Turn radii of the sharpest turns averaged 0.14 m, which was 0.24 L. These turns had a mean length-specific speed of 2.22 L/s. Turning rate for the penguins ranged from 57.9 to 545.8 ^{o}/s, with a mean turning rate of 232 ^{o}/s.

e. Cephalopod maneuvering

Turning rates by squid are considered slow at 2 s to execute a 180^{o} turn [67]. Squids, which keep the mantle stiff, cannot produce turns of less than 0.5*L* [67]. Squids show considerable lateral side-slip when undergoing body rotation [67]. The shelled *Nautilus* can at best negotiate a turn of 2*L* [176], which is equivalent to submarines with inflexible hulls and turning radii of 2-3*L* [63].

f. Sea turtle maneuvering

Sea turtles can turn by either forelimb movements alone, or by a combination of forelimb and hind limb movements [116]. Asynchronous movements of the forelimbs of sea turtles are used to turn [8]. The duration of the flapping movements in leatherback sea turtles are shorter for the forelimb on the inside of the turn. In hatchling loggerhead turtles, both forelimb and hind limbs are used for turning [6], [177]. The broad hind limbs of sea turtles act as rudders [116], [178]. The lack of fusion of the ankle bones has been assumed to aid in fine adjustment of the rudder [178].

CONCLUSIONS

The large array of biological control surfaces for non-piscine vertebrates and cephalopods can be divided into two fundamental structures, paddles and wing-like flippers. For paddles, the major force generated is drag, whereas for the flippers, the major force is lift. To effectively generate drag, paddles have a relatively flat cross-section with a broad , low aspect ratio planform and narrow articulated base. Flippers, also including cetacean flukes and dorsal fins, have a relatively high aspect ratio and foil-like cross-section. The cross-sectional geometry suggests the ability to enhance lift production with low drag and delayed stall at high angles of attack. Performance data show that wing-like flippers are used in small radius turns at high rates. Drag-based paddles would be effective in maneuvering at low speeds in confined spaces.

REFERENCES

[1] J. M. Gal and R. W. Blake, "Biomechanics of frog swimming. I. Estimation of the propulsive force generated by *Hymenochirus boettgeri*," *J. Exp. Biol.* vol. 138, pp. 399-411, 1988.

[2] J. M. Gal and R. W. Blake, "Biomechanics of frog swimming. II. Mechanics of the limb-beat cycle in *Hymenochirus boettgeri*," *J. Exp. Biol.* vol. 138, pp. 413-429, 1988b.

[3] G. R. Zug, 'Buoyancy, locomotion, morphology of the pelvic girdle and hindlimbs, and systematics of cryptodiran turtles," *Misc. Publ. Mus. Zool. Univ. Mich.* vol. 142, pp. 1-98, 1971.

[4] P. S. G. Stein, "Swimming movements elicited by electrical stimulation of the turtle spinal cord: the high spinal preparation," *J. Comp. Physiol.* vol. 124, pp. 203-210, 1978.

[5] W. F. Walker, Jr. "Swimming in sea turtles of the family Cheloniidae," *Copeia* vol. 1971, pp. 229-233, 1971.

[6] J. Davenport and W. Clough, "Swimming and diving in young loggerhead sea turtles (*Caretta caretta* L.)," *Copeia* vol. 1986, pp. 53-57, 1986.

[7] J. Davenport, "Locomotion in hatchling leatherback turtles *Dermochelys coriacea*," *J. Zool., Lond.* vol. 212, pp. 85-101, 1987.

[8] S. Renous and V. Bels, "Comparison between aquatic and terrestrial locomotions of the leatherback sea turtle (*Dermochelys coriacea*)," *J. Zool., Lond.* vol. 230, pp. 357-378, 1993.

[9] J. A. Massare, "Swimming capabilities of Mesozoic marine reptiles: implications for method of predation," *Paleobiology*, vol. 14, pp. 187-205, 1988.

[10] J. A. Massare, "Swimming capabilities of Mesozoic marine reptiles: a review," in *Mechanics and Physiology of Animal Swimming*, Q. Bone, L. Maddock and J. M. V. Rayner, Eds. Cambridge: Cambridge University Press, 1994, pp. 133-149.

[11] A. B. Howell, *Aquatic Mammals*. Springfield, Illinois: Charles C. Thomas, 1930.

[12] J. Lighthill, "Hydrodynamics of aquatic animal propulsion - a survey," *Ann. Rev. Fluid Mech*. vol. 1, pp. 413-446, 1969.

[13] M. Taylor, "Reptiles that took on the sea," *New Sci.*, vol. 26, pp. 48-51, 1987.

[14] R. Motani, "Scaling effects in caudal fin propulsion and the speed of ichthyosaurs," *Nature*, vol. 415, pp. 309-312, 2002.

[15] R. Motani, "Swimming speed estimation of extinct marine reptiles: energetic approach revisited," *Paleobiology*, vol. 28, pp. 251-262, 2002.

[16] R. C. Osburn, "Adaptive modifications of the limb skeleton in aquatic reptiles and mammals," *Annals N. Y. Acad. Sci.*, vol. 16, pp. 447-482, 1906.

[17] J. A. Robinson, "The locomotion of plesiosaurs," *N. Jb. Geol. Paläont., Abh.*, vol. 149, pp. 286-332, 1975.

[18] S. Tarsitano and J. Riess, "Plesiosaur locomotion – underwater flight versus rowing," *N. Jb. Geol. Paläont., Abh.*, vol. 164, pp. 188-192, 1982.

[19] S. J. Godfrey, "Plesiosaur subaqueous locomotion a reappraisal," *N. Jb. Geol. Paläont., Mh.*, vol. 11, pp. 661-672, 1984.

[20] J. Riess, Fortbewegunsweise, "Schwimmbiophysik und Phylogenie der Ichthyosaurier," *Palaeontographica A*, vol. 192, pp. 93-155, 1986.

[21] Baudinette, R. V. and Gill, P. 1985. The energetics of 'flying' and 'paddling' in water: locomotion in penguins and ducks. J. Comp. Physiol. B 155: 373-380.

[22] T. L. Aigeldinger and F. E. Fish, "Hydroplaning by ducklings: Overcoming limitations to swimming at the water surface," *J. Exp. Biol.*, vol. 198, pp. 1567-1574, 1995.

[23] F. E. Fish, "Kinematics of ducklings swimming in formation: Energetic consequences of position," *J. Exp. Zool*., vol. 272, pp. 1-11, 1995.

[24] J. M. V. Rayner, "Vorticity and propulsion mechanics in swimming and flying animals," in *Konstruktionsprinzipen lebender und ausgestorbener Reptilien* J. Riess and E. Frey, Eds. Tubingen, F.R.G.: University of Tubingen, 1985, pp. 89-118.

[25] B. D. Clark and W. Bemis, "Kinematics of swimming of penguins at the Detroit Zoo," *J. Zool., Lond*., vol. 188, pp. 411-428, 1979.

[26] C. A. Hui, "Penguin swimming. I. Hydrodynamics," *Physiol. Zool.*, vol, 61, pp. 333-343, 1988.

[27] C. A. Hui, "Penguin swimming. II. Energetics and behavior," *Physiol. Zool*. vol. 61, pp. 344-350, 1988.

[28] R. Bannasch, "Functional anatomy of the 'flight' apparatus in penguins," in *Mechanics and Physiology of Animal Swimming,* Q. Bone, L. Maddock and J. M. V. Rayner, Eds. Cambridge: Cambridge University Press, 1994, pp. 163-192.

[29] R. Bannasch, "Hydrodynamics of penguins - an experimental approach," in *The Penguins: Ecology and Management*. P. Dann, I. Norman and P. Reilly, Eds. Norton, NSW: Surrey Beatty and Sons, 1995, pp. 141-176.

[30] F. E. Fish, "Influence of hydrodynamic design and propulsive mode on mammalian swimming energetics," *Aust. J. Zool.*, vol. 42, pp. 79-101, 1993.

[31] A. B. Crowther, "On some points of interest connected with the platypus," *Pap. Proc. Roy. Soc. Tas*. pp. 96-99, 1879.

[32] H. Burrell, *The Platypus*. Sydney: Angus & Robertson, 1927..

[33] J. D. Mizelle, "Swimming of the muskrat," *J. Mamm.*, vol. 16, pp. 22-25, 1935.

[34] A. B. Howell, "The swimming mechanism of the platypus," *J. Mamm.*, vol. 18, pp. 217-222, 1937..

[35] T. M. Williams, "Locomotion in the North American mink, a semi-aquatic mammal. I. Swimming energetics and body drag," *J. Exp. Biol.*, vol. 103, pp. 155-168, 1983.

[36] F. E. Fish, "Mechanics, power output, and efficiency of the swimming muskrat (*Ondatra zibethicus*)," *J. Exp. Biol*., vol. 110, pp. 183-201, 1984.

[37] F. E. Fish, R. V. Baudinette, P. B. Frappell, and M. P. Sarre, "Energetics of swimming by the platypus *Ornithorhynchus anatinus*: metabolic effort associated with rowing," *J. Exp. Biol*., vol. 200, pp. 2647-2652, 1997.

[38] F. E. Fish, "Association of propulsive swimming mode with behavior in river otters (*Lutra canadensis*)," *J. Mamm.*, vol. 75, pp. 989-997, 1994.

[39] S. D. Feldkamp, Swimming in the California sea lion: Morphometrics, drag and energetics. *J. Exp. Biol*., vol. 131, pp. 117-135, 1987.

[40] S. D. Feldkamp, Foreflipper propulsion in the California sea lion, *Zalophus californianus*. *J. Zool., Lond.*, vol. 212, pp. 43-57, 1987.

[41] F. E. Fish, S. Innes, and K. Ronald, "Kinematics and estimated thrust production of swimming harp and ringed seals," *J. Exp. Biol.*, vol. 137, pp. 157-173, 1988.

[42] F. E. Fish, "Transitions from drag-based to lift-based propulsion in mammalian swimming," *Amer. Zool*., vol. 36, pp. 628-641, 1996.

[43] F. E. Fish, Imaginative solutions by marine organisms for drag reduction.. in *Proceedings of the International Symposium on Seawater Drag Reduction*, J. C. S. Meng, Ed. Newport, Rhode Island, 1998, pp. 443-450.

[44] F. E. Fish, "Biomechanical perspective on the origin of cetacean flukes," In *The Emergence of Whales: Evolutionary Patterns in the Origin of Cetacea*, J. G. M. Thewissen, Ed. New York: Plenum Press, 1998, pp. 303-324.

[45] F. E. Fish, and J. Rohr, "Review of dolphin hydrodynamics and swimming performance," *SPAWARS System Center Technical Report* 1801, San Diego, CA. 1999. http://www.spawar.navy.mil/sti/publications/pubs/tr/1801/tr1801.pdf

[46] S. J. Godfrey, "Additional observations of subaqueous locomotion in the California Sea Lion (*Zalophus californianus*)," *Aqu. Mamm*., vol. 11, pp.53-57, 1985.

[47] D. A. Parry, "Anatomical basis of swimming in whales," *Proc. Zool. Soc. Lond*., vol. 119, pp. 49-60, 1949.

[48] D. S. Hartman, "Ecology and behavior of the manatee (*Trichechus manatus*) in Florida," *Spec. Publ. Amer. Soc. Mamm*., No. 5, 1979.

[49] T. G. Lang and D. A. Daybell, "Porpoise performance tests in a seawater tank," *Nav. Ord. Test Sta. Tech. Rep.* 3063, 1963..

[50] M. Nishiwaki and H. Marsh, "Dugong - Dugong dugon (Muller, 1776)," in *Handbook of Marine Mammals*, Vol. 3, S. H. Ridgway and R. Harrison, Eds. London: Academic Press, 1985, pp. 1-31.

[51] J. Videler and P. Kamermans, "Differences between upstroke and downstroke in swimming dolphins," *J. Exp. Biol.*, vol. 119, pp. 265-274, 1985.

[52] K. M. Backhouse, Locomotion of seals with particular reference to the forelimb. *Symp. Zool. Soc. Lond*., vol. 5, pp. 59-75, 1961.
[53] G. C. Ray, "Locomotion in pinnipeds," *Nat. Hist*., vol. 72, pp. 10-21, 1963.
[54] F. J. Tarasoff, A. Bisaillon, J. Pierard, and A. P. Whitt, "Locomotory patterns and external morphology of the river otter, sea otter, and harp seal (Mammalia)," *Can. J. Zool*., vol. 50, pp. 915-929, 1972..
[55] K. R. Gordon, "Locomotor behaviour of the walrus (*Odobenus*)," *J. Zool., Lond*., vol. 195, pp. 349-367, 1981.
[56] P. W. Webb, "Hydrodynamics and energetics of fish propulsion," *Bull. Fish. Res. Bd. Can.*, vol. 190, pp. 1-158, 1975.
[57] C. C. Lindsey, "Form, function, and locomotory habits in fish," in *Fish Physiology: Locomotion*, Vol. 7, W. S. Hoar and D. J. Randall, Eds. New York: Academic Press, 1978, pp. 1-100.
[58] G. J. D. Smith, K. W. Browne, and D. E. Gaskin, Functional myology of the harbour porpoise, *Phocoena phocoena* (L.). *Can. J. Zool.,* vol. 54, pp. 716-729, 1976.
[59] Y. G. Aleyev, *Nekton*. The Hague: Junk, 1977.
[60] R. K. Edel and H. E. Winn, "Observations on underwater locomotion and flipper movement of the humpback whale *Megaptera novaeangliae*," *Mar. Biol*., vol. 48, pp. 279-287, 1978.
[61] M. Klima, H. A. Oelschläger, and D. Wünsch, "Morphology of the pectoral girdle in the Amazon dolphin *Inia geoffrensis* with special reference to the shoulder joint and the movements of the flippers," *Z. Saugertierkunde*, vol. 45, pp. 288-309, 1987.
[62] F. E. Fish, "Balancing requirements for stability and maneuverability in cetaceans," *Integ. Comp. Biol.*, vol. 42, pp. 85-93, 2002.
[63] N. K. Maslov, "Maneuverability and controllability of dolphins," *Bionika* vol. 4, pp. 46-50, 1970. (translated from Russian).
[64] F. E. Fish, "Swimming mode changes associated with terrestrial-semiaquatic transition in mammals," *Amer. Zool*., vol. 27, pp. 86A, 1987.
[65] D. P. Domning and V. de Buffrenil, "Hydrostasis in the Sirenia: quantitative data and functional interpretation," *Mar. Mamm. Sci*., vol. 7, pp. 331-368, 1991.
[66] R. K. O'Dor, "Limitations on locomotor performance in squid," *J. Appl. Physiol*., vol. 64, pp. 128-134, 1988..
[67] T. P. Foyle, and R. K. O'Dor, "Predatory strategies of squid *(Illex illecebrosus*) attacking small and large fish," *Mar. Behav. Physiol*., vol. 13, pp. 155-168, 1988.
[68] A. Azuma, *The Biokinetics of Flying and Swimming*. Tokyo: Springer-Verlag, 1992.
[69] P. W. Webb and R. W. Blake, "Swimming," in *Functional Vertebrate Morphology*, M. Hildebrand, D. M. Bramble, K. F. Liem, and D. B. Wake, Eds. Cambridge: Harvard Univ. Press, 1985, pp. 110-128.
[70] P. W. Webb, "Simple physical principles and vertebrate aquatic locomotion," *Amer. Zool.*, vol. 28, pp. 709-725, 1988.
[71] T. Daniel, C. Jordan, and D. Grunbaum, "Hydromechanics of swimming," In *Advances in Comparative & Environmental Physiology 11: Mechanics of Animal Locomotion*, R. McN. Alexander, Ed. Berlin: Springer-Verlag, 1992. pp. 17-49.
[72] R. McN. Alexander, "The history of fish mechanics," in *Fish Biomechanics*, P. W. Webb and D. Weihs, Eds. Praeger, New York, 1983, pp. 1-35.
[73] R. W. Blake, *Fish Locomotion*. Cambridge: Cambridge University Press, 1983.
[74] R. W. Blake, "The mechanics of labriform locomotion. I. Labriform locomotion in the angelfish (*Pterophyllum eimekei*): an analysis of the power stroke," *J. Exp. Biol*., vol. 82, pp. 255-271, 1979.
[75] T. L. Daniel, "Unsteady aspects of aquatic locomotion," *Amer. Zool*., vol. 24, pp. 121-134, 1984..
[76] T. L. Daniel and P. W. Webb, "Physics, design, and locomotor performance," in *Comparative Physiology: Life in Water and on Land*, P. Dejours, L. Bolis, C. R. Taylor and E. R. Weibel, Eds. New York: Liviana Press, Springer-Verlag, 1987, pp. 343-369.
[77] V. I. Arreola, and M. W. Westneat, "Mechanics of propulsion by multiple fins: kinematics of aquatic locomotion in the burrfish (*Chilomycterus schoepfi*)," *J. Exp. Biol*., vol. 263, pp. 1689-1696, 1996.
[78] J. Lighthill, *Mathematical Biofluiddynamics*. Philadelphia: Soc. Indust. Appl. Math., 1975..
[79] P. W. Webb, "Hydrodynamics: Nonscombrid fish," in *Fish Physiology: Locomotion*, Vol. VII, W. S. Hoar and D. J. Randall, Eds. New York: Academic Press, 1978, pp. 189-237.
[80] C. R. Tracy and K. A. Christian, "Are marine iguana tails flattened?," *Brit. J. Herp*., vol. 6, pp. 434-435, 1985.
[81] P. W. Webb, "Form and function in fish swimming," *Sci. Amer*., vol. 251, pp. 72-82, 1984.
[82] C. P. van Dam, "Efficiency characteristics of crescent-shaped wings and caudal fins.," *Nature*, vol. 325, pp. 435-437, 1987.
[83] D. Weihs and P. W. Webb. "Optimization of locomotion," in *Fish Biomechanics*, P. W. Webb and D. Weihs, Eds. New York: Praeger, 1983, pp. 339-371.
[84] H. L. Fierstine, and V. Walters, "Studies of locomotion and anatomy of scombrid fishes," *Mem. S. Calif. Acad. Sci.*, vol. 6, pp. 1-31, 1968.
[85] J. J. Magnuson, "Locomotion by scombrid fishes: hydrodynamics, morphology and behaviour," in *Fish physiology*, vol. 7, W. S. Hoar and D. J. Randall, Eds. London: Academic Press, 1978, pp. 239-313.
[86] F. E. Fish, "Power output and propulsive efficiency of swimming bottlenose dolphins (*Tursiops truncatus*)," *J. Exp. Biol*., vol. 185, pp.179-193, 1993.
[87] F. E. Fish and L.D. Shannahan, "Comparative shark locomotion in relation to body and pectoral fin angles," *J. Fish Biol*., vol. 56, pp. 1062-1073, 2000.
[88] S. Vogel, *Life in Moving Fluids*. Princeton: Princeton University Press, 1994.
[89] R. H. Barnard and D. R. Philpott, *Aircraft Flight*. Essex: Longman Scientific &Technical, 1995..
[90] H. C. Smith, *Illustrated Guide to Aerodynamics*. Blue Ridge Summit, PA: McGraw-Hill, 1992.
[91] D. Weihs, "Stability of aquatic animal locomotion," *Cont. Math.,* vol. 141, pp. 443-461, 1993..
[92] J. E. Harris, "The role of the fins in the equilibrium of the swimming fish. I. Wind-tunnel tests on a model of *Mustelus canis* (Mitchill)," *J. Exp. Biol*., vol. 13, pp. 476-493, 1936.
[93] J. E. Harris, "The mechanical significance of the position and movements of the paired fins in the Teleostei," *Pap. Tortugas Lab*., vol. 31, pp. 173-189, 1937.
[94] J. E. Harris, "The role of the fins in the equilibrium of the swimming fish. II. The role of the pelvic fins," *J. Exp. Biol*., vol. 15, pp. 32-47, 1938.
[95] P. W. Webb, "Speed, acceleration and manoeuvrability of two teleost fishes," *J. Exp. Biol*., vol. 102, pp. 115-122, 1983.
[96] P. W. Webb, Designs for stability and maneuverability in aquatic vertebrates: What can we learn? *Proceedings of the Tenth International Symposium on Unmanned Untethered Submersible Technology: Proceedings of the Special Session on Bio-Engineering Research Related to Autonomous Underwater Vehicles*, Autonomous Undersea Systems Institute, Lee, New Hampshire, 1997, pp. 86-103.
[97] P. W. Webb, "Control of posture, depth, and swimming trajectories of fishes," *Integ. Comp. Biol.*, vol. 42, pp. 94-101, 2002.
[98] D. Weihs, "Design features and mechanics of axial locomotion in fish," *Amer. Zool*., vol. 29, pp. 151-160, 1989..
[99] D. Weihs, "Stability versus maneuverability in aquatic locomotion," *Integ. Comp. Biol*., vol. 42, pp. 127-134, 2002.
[100] P. W. Webb, G. D. LaLiberte, and A. J. Schrank, "Does body and fin form affect the maneuverability of fish traversing vertical and horizontal slits," *Environ. Biol. Fish*., vol. 46, pp. 7-14, 1996.
[101] F. E. Fish, "Biological designs for enhanced maneuverability: Analysis of marine mammal performance," in *Tenth International Symposium on Unmanned Untethered Submersible Technology: Proceedings of the Special Session on Bio-Engineering Research Related to Autonomous Underwater Vehicles*. Autonomous Undersea Systems Institute, Durham, New Hampshire, 1997, pp. 109-117.
[102] F. E. Fish, "Performance constraints on the maneuverability of flexible and rigid biological systems," in *Proceedings of the Eleventh International Symposium on Unmanned Untethered Submersible Technology*, Autonomous Undersea Systems Institute, Lee, New Hampshire, 1999, pp. 394-406.

[103] P. P. Wegener, "*What Makes Airplanes Fly?*" New York: Springer-Verlag, 1991.

[104] P. R. Bandyopadhyay, J. M. Castano, J. Q. Rice, R. B. Philips, W. H. Nedderman, and W. K. Macy. "Low-speed maneuvering hydrodynamics of fish and small underwater vehicles," *Trans. ASME*, vol. 119, pp. 136-144, 1997.

[105] P. R. Bandyopadhyay and M. J. Donnelly, "The swimming hydrodynamics of a pair of flapping foils attached to a rigid body," in *Tenth Internat. Symp. Unmanned Untethered Submersible Tech.: Proc. Sp. Ses. Bio-Eng Res. Related to Autonomous Underwater Vehicles,* Autonomous Undersea Systems Institute, Lee, NH, 1997, pp. 27-43.

[106] C. M., Breder, Jr., "On structural specialization of flying fishes from the standpoint of aerodynamics," *Copeia*, vol. 1930, pp. 114-121, 1930.

[107] H. H., Hurt, Jr., *Aerodynamics for Naval Aviators*. U. S. Navy, NAVWEPS 00-80T-80, 1965.

[108] D. F. Anderson and S. Eberhardt, *Understanding Flight*. New York: McGraw Hill, 2001.

[109] J. A. Walker, "Does a rigid body limit maneuverability?," *J. Exp. Biol*., vol. 203, pp. 3391-3396, 2000.

[110] P. W. Webb, "Is the high cost of body/caudal fin undulatory swimming due to increased friction drag or inertial recoil." *J. Exp. Biol*., vol. 162, pp.157-166, 1992.

[111] F. E. Fish, "Function of the compressed tail of surface swimming muskrats (*Ondatra zibethicus*)," *J. Mamm.*, vol. 63, pp. 591-597, 1982.

[112] L. A. Ferry and G. V. Lauder, "Heterocercal tail function in leopard sharks: a three-dimensional kinematic analysis of two models," *J. Exp. Biol*., vol. 199, pp. 2253-2268, 1996.

[113] W. J. L. Felts, "Some functional and structural characteristics of cetacean flippers and flukes," in *Whales, Dolphins, and Porpoises*, K. S. Norris, Ed. Berkeley: University of California Press, 1966, pp. 255-276.

[114] A. W. English, "Structural correlates of forelimb function in fur seals and sea lions," J. Morph., vol. 151, pp. 325-352, 1977.

[115] G. D. Fitzgerald, "Comparative morphology of the forelimb skeleton in some Odontoceti (Mammalia, Cetacea)," M.A. thesis. California State College, Long Beach, 1970.

[116] J. Wyneken, "Sea turtle locomotion: mechanisms, behavior, and energetics," in *The biology of sea turtles*, P. L. Lutz and J. A. Musick Eds. Boca Raton: CRC Press, 1997, pp. 165-198.

[117] E. J. Slijper, *Whales* Ithaca, New York: Cornell University Press, 1979.

[118] J. G. M. Thewissen and F. E. Fish, "Locomotor evolution in the earliest cetaceans: Functional model, modern analogues, and paleontological evidence," *Paleobiology*, vol. 23, pp. 482-490, 1997.

[119] A. W. English, "Limb movements and locomotor function in the California sea lion (*Zalophus californianus*)," *J. Zool., Lond.*, vol. 178, pp. 341-364, 1976.

[120] P. E. Purves and G. Pilleri, "The functional anatomy and general biology of *Pseudorca crassidens* (Owen) with a review of the hydrodynamics and acoustics," in Cetacea. in *Investigation on Cetacea* Vol. IX, G. Pilleri, Ed. Bern Switzerland: Institute of Brain Anatomy, 1978, pp. 68-227.

[121] J. E. Heyning, "Cuvier's beaked whale Ziphius cavirostris," in *Encyclopedia of Marine Mammals*. W. F. Perrin, B. Würsig, and J. G. M. Thewissen, Eds. San Diego: Academic Press, 2002, pp. 305-307.

[122] G. I. Vasilevskaya, "Structural features of the delphinid pectoral flippers," *Bionika*, vol. 8, pp. 127-132, 1974. (translated from Russian).

[123] G. Pilleri, M. Gihr, P. E. Purves, K. Zbinden, and C. Kraus, "On the behaviour, bioacoustics and functional morphology of the Indus River dolphin (*Platanista indi* Blyth, 1859)," *Invest. Cetacea*, vol. 6, pp. 11-141, 1976.

[124] C. M. Jurasz and V. P. Jurasz, "Feeding modes of the humpback whale, *Megaptera novaeangliae*, in southeast Alaska," *Sci. Rep. Whales Res. Inst.*, vol. 31, pp. 69-83, 1979.

[125] F. E. Fish and J. M. Battle, "Hydrodynamic design of the humpback whale flipper," *J. Morph.*, vol. 225, pp. 51-60, 1995.

[126] F. W. True, *The Whalebone Whales of the Western North Atlantic*. Washington, D.C.: Smithsonian Institution Press, 1983.

[127] A. G. Tomilin, *Mammals of the U.S.S.R. and Adjacent Countries,* Vol. IX, *Cetacea*. Moskva: Izdatel'stvo Akademi Nauk SSSR, 1957.

[128] L. K. Winn and H. E. Winn, *Wings in the Sea: The Humpback Whale*. Hanover: University Press of New England, 1985.

[129] S. M. Minasian, K. C. Balcomb, III, and L. Foster. *The World's Whales*. Washington, D. C.: Smithsonian Books, 1984.

[130] H. E. Winn, and B. L. Olla. *Behavior of Marine Animals'*, Vol. 3. New York: Plenum Press, 1979.

[131] S. F. Hoerner, *Fluid-Dynamic Drag*. Brick Town, New Jersey: Published by author, 1965..

[132] R. W. Blake, "Influence of pectoral fin shape on thrust and drag in labriform locomotion," *J. Zool., Lond*., vol. 194, pp. 53-66, 1981.

[133] F. E. Fish, J. Hurley, and D. P. Costa, "Maneuverability by the sea lion, *Zalophus californianus*: Turning performance of an unstable body design," *J. Exp. Biol.*, vol. 206, pp. 667-674, 2003.

[134] T. G. Lang, "Hydrodynamic analysis of dolphin fin profiles," *Nature* vol. 209, pp. 1110-1111, 1966..

[135] S. V. Pershin, *Fundamentals of Hydrobionics*. Leningrad: Sudostroyeniye Publ., 1988. (translated from Russian).

[136] R. von Mises, *Theory of Flight*. New York: Dover, 1945.

[137] J. Lighthill, "Introduction to scaling of aerial locomotion," in *Scale Effects in Animal Locomotion*, T. J. Pedley, Ed. London: Academic Press, 1977, pp. 365-404.

[138] W. Y. Yasui, "Morphometrics, hydrodynamics and energetics of locomotion for a small cetacean, *Phocoena phocoena* (L.)," M. Sc. thesis, Univ. of Guelph, Ontario, 1980.

[139] T. G. Lang, and K. Pryor. "Hydrodynamic performance of porpoises (*Stenella attenuata*)," *Science*, vol. 152, pp. 531-533, 1966..

[140] D. Küchermann, "The distribution of lift over the surface of swept wings," *Aero. Quart*., vol. 4, pp. 261-278, 1953.

[141] J. Ashenberg, and D. Weihs, "Minimum induced drag of wings with curved planform," *J. Aircraft*, vol. 21, pp. 89-91, 1984.

[142] P. Liu and N. Bose, "Propulsive performance of three naturally occurring oscillating propeller planforms," *Ocean Eng*., vol. 20, pp. 57-75, 1993.

[143] N. Bose, J. Lien, and J. Ahia, "Measurements of the bodies and flukes of several cetacean species," *Proc. Roy. Soc. Lond. B*, vol. 242, pp. 163-173, 1990..

[144] T. L. Daniel, "Forward flapping flight from flexible fins," *Can. J. Zool*., vol. 66, pp. 630-638, 1988.

[145] G. A. Stevens, "Swimming of dolphins," *Sci. Prog*., vol. 38, pp. 524-525, 1950.

[146] F. G. Wood, *Marine Mammals and Man: The Navy's Porpoises and Sea Lions*. Washington: Robert B. Luce, 1973.

[147] J. W. Fitzgerald, "Artificial dolphin blubber could increase sub speed, cut noise," *Navy News Undersea Tech.*, vol. 9, pp. 1-2, 1991.

[148] M. I. Latz, J. Rohr, and J. Hoyt, "A novel flow visualization technique using bioluminescent marine plankton - Part I: Laboratory studies," *IEEE J. Ocean. Eng*., vol. 20, pp. 144-147, 1995.

[149] J. Rohr, M. I. Latz, S. Fallon, J. C. Nauen, and E. Hendricks, "Experimental approaches towards interpreting dolphin-stimulated bioluminescence," *J. Exp. Biol.*, vol. 201, pp. 1447-1460, 1998.

[150] D. M. Bushnell and K. J. Moore, "Drag reduction in nature," *Ann. Rev. Fluid Mech*., vol. 23, pp. 65-79, 1991.

[151] U. M. Norberg, *Vertebrate Flight*. Berlin: Springer-Verlag, 1990.

[152] R. S. Shevell, "Aerodynamic anomalies: Can CFD prevent or correct them?," *J. Aircraft*, vol. 23, pp. 641-649, 1986.

[153] P. Watts and F. E. Fish, "The influence of passive, leading edge tubercles on wing performance," in *Proceedings of the Twelfth International Symposium on Unmanned Untethered Submersible Technology*. Autonomous Undersea Systems Institute, Durham New Hampshire, 2001.

[154] P. W. Bearman, and J. C. Owen, "Reduction of bluff-body drag and suppression of vortex shedding by the introduction of wavy separation lines," *J. Fluids Struct*., vol. 12, pp. 123-130, 1998.

[155] J. C. Owen, A. A. Szewczyk, and P. W. Bearman, "Suppression of Karman vortex shedding," *Phys. Fluids*, vol. 12, pp. S9, 2000.

[156] C. A. Hui, "Maneuverability of the Humboldt penguin (*Spheniscus humboldti*) during swimming," *Can. J. Zool.*, vol. 63, pp. 2165-2167, 1985.

[157] H. C. Howland, "Optimal strategies for predator avoidance: The relative importance of speed and manoeuvrability," *J. Theor. Biol*., vol. 47, pp. 333-350, 1974.

[158] D. Weihs, "Effects of swimming path curvature on the energetics of fish motion," *Fish. Bull.*, vol. 79, pp. 171-179, 1981.

[159] P. Domenici and R. W. Blake, "The kinematics and performance of the escape in the angelfish (*Pterophyllum eimekei*)," *J. Exp. Biol.*, vol. 156, pp. 187-205, 1991.

[160] P. F. Brodie, "The white whale *Delphinapterus leucas* (Pallas, 1776)," in *Handbook of Marine Mammals*, Vol. 4, S. H. Ridgway and R. Harrison, Eds. London: Academic Press, 1989, pp. 119-144.

[161] C. L. Gerstner, "Maneuverability of four species of coral-reef fish that differ in body and pectoral-fin morphology," *Can. J. Zool*., vol. 77, pp. 1102-1110, 1999.

[162] J. L. Holak, F. E. Fish, D. P. Nowacek, and S. M. Nowacek, "High performance turning capabilities during foraging by bottlenose dolphins (*Tursiops truncatus*)," *Integ. Comp. Biol*., in press, 2002.

[163] P. W. Webb, "The effect of size on the fast-start performance of rainbow trout. *Salmo gairdneri*, and a consideration of piscivorous predator-prey interactions," *J. Exp. Biol.,* vol. 65, pp. 157-177, 1976.

[164] D. Miller, *Submarines of the World*. New York: Orion Books, 1991.

[165] R. W. Blake, L. M. Chatters, and P. Domenici, "Turning radius of yellowfin tuna (*Thunnus albacares*) in unsteady swimming manoevres," *J. Fish Biol.*, vol. 46, pp. 536-538, 1995..

[166] F. J. Hester, J. R. Hunter, and R. R. Whitney, "Jumping and spinning behavior in the spinner dolphin," *J. Mamm*., vol. 44, pp. 586-588, 1963.

[167] M. Riedman, *The Pinnipeds: Seals, Sea Lions, and Walruses*. Berkeley: University of California Press, 1990.

[168] R. S. Peterson and G. A. Bartholomew, *The Natural History and Behavior of the California Sea Lion*. Sp. Publ. No. 1, Amer. Soc. Mamm., 1967.

[169] M. Nishiwaki, "General biology," in *Mammals of the Sea: Biology and Medicine*, S. H. Ridgway, Ed. Springfield, Illinois: C. C. Thomas, 1972, pp. 3-204.

[170] C. J. Madsen, and L. M. Herman, "Social and ecological correlates of cetacean vision and visual appearance," in *Cetacean Behavior: Mechanisms and Functions,* L. M. Herman, Ed. Malabar, Florida: R. E. Krieger Publ., 1980, pp. 101-147.

[171] H. E., Winn, and N. E. Reichley, "Humpback whale Megaptera novaeangliae (Borowski, 1781)," in *Handbook of Marine Mammals,* Vol. 3: *The Sirenians and Baleen Whales*, S. H. Ridgway, and R. Harrison, Eds. London: Academic Press, 1985, pp. 241-273.

[172] W. F. Dolphin, "Foraging dive patterns of humpback whales, *Megaptera novaeangliae*, in southeast Alaska: cost-benefit analysis," *Can J. Zool*., vol. 66, pp. 2432-2441, 1988.

[173] J. H. W. Hain, G. R. Carter, S. D. Kraus, C. A. Mayo, and H. E. Winn, "Feeding behavior of the humpback whale, *Megaptera novaeangliae*, in the western North Atlantic," *Fish. Bull*., vol. 80, pp. 259-268, 1982.

[174] F. A. Sharpe, and L. M. Dill, "The behavior of Pacific herring schools in response to artificial humpback whale bubbles," *Can J. Zool*., vol. 75, pp. 725-730, 1997.

[175] A. Ingebrigtsen, "Whales caught in the North Atlantic and other seas," *Rapp. P.-V. Reun. Cons. Int. Explor. Mer.*, vol. 56, pp. 1-26, 1929.

[176] J. A. Chamberlain, Jr., "Jet propulsion of *Nautilus*: a surviving example of early paleozoic cephalopod locomotor design," *Can. J. Zool*., vol. 68, pp. 806-814, 1990.

[177] K. J. Lohmann, A. W. Swartz, and C. M. F. Lohmann, "Perception of ocean wave direction by sea turtles," *J. Exp. Biol.*, vol. 198, pp. 1079-1083, 1995..

[178] W. F. Walker, Jr., "The locomotor apparatus of testudines," in *Biology of Reptilia*, Vol. 4, *Morphology* D, C. Gans and T. S. Parsons, Eds. London: Academic Press, 1973, pp. 1-100.

[179] T. G. Lang, "Speed, power, and drag measurements of dolphins and porpoises," in *Swimming and Flying in Nature*, Vol. 2, T. Y. Wu, C. J. Brokaw and C. Brennen, Eds. New York: Plenum Press, 1975, pp. 553-571.

[180] F. E. Fish and D. R. Ketten, "Examination of three-dimensional geometry of cetacean flukes using CT-scans," *Integ. Comp. Biol.*, In press, 2002.